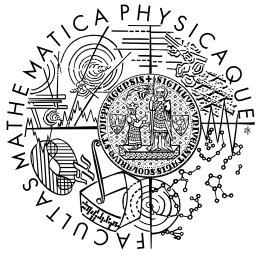

FACULTY
OF MATHEMATICS
AND PHYSICS
Charles University

BACHELOR THESIS

Tobiáš Krupa

SP_n approximation to the radiative heat transport equation

Mathematical Institute of Charles University

Supervisor of the bachelor thesis: RNDr. Ondřej Souček, Ph.D.
Study programme: Mathematics
Study branch: Mathematical modeling

Prague 2023

I declare that I carried out this bachelor thesis independently, and only with the cited sources, literature and other professional sources. It has not been used to obtain another or the same degree.

I understand that my work relates to the rights and obligations under the Act No. 121/2000 Sb., the Copyright Act, as amended, in particular the fact that the Charles University has the right to conclude a license agreement on the use of this work as a school work pursuant to Section 60 subsection 1 of the Copyright Act.

In ..... date ....

Author's signature

I would like to thank my supervisor RNDr. Ondřej Souček, Ph.D. I am grateful for his numerous advice which kept me on the right path and also willingness to consult every minor problem or partial result. His guidance has made this work a pleasure and I feel that I have learnt a lot from him.

I must appreciate the help from my consultants RNDr. Karel Tůma, Ph.D. and Mgr. Vít Průša, Ph.D. regarding used software.

I am also grateful to my family for fully supporting me during my studies at Charles University. You are always there for me, thank you.

Finally, I would like to thank everybody who has helped me in anyway throughout my studies and especially during the last couple of months. I sincerely appreciate it.

Title: SP_n approximation to the radiative heat transport equation

Author: Tobiáš Krupa

Institute: Mathematical Institute of Charles University

Supervisor: RNDr. Ondřej Souček, Ph.D., Mathematical Institute of Charles University

Abstract: This thesis is dedicated to a problem of heat transport where radiation is taken into account. Models for such setting, although complicated, are very important for industrial purposes.

We provide a derivation and explanation of the fundamental physical model for radiative heat transport. The resulting system of radiative transfer equations (RTE) is then approximated with so-called SP_n equations. Here, we focus on asymptotically deriving a simple set of SP_1 equations. Special attention is given to Marsak-type boundary conditions which we formulate in a more precise form than other sources.

Inspired by the float-glass forming process, we look into problems with multiple domains with different refractive indices. For such an arrangement, there is a need for transition conditions describing the behaviour of the solutions on the interface between two domains of interest. By following an analogous procedure as for the boundary conditions, we have managed to identify a natural set of transition conditions that allow for discontinuity in the intensity variable. To our best knowledge, these conditions have not been yet presented in the literature.

Finally, we present several numerical experiments of solving these equations in *Wolfram Mathematica* software and compare them with benchmark results.

Keywords: radiative heat transport, SPn approximation, boundary conditions, transition conditions

Název práce: SP_n aproximace rovnice radiačního přenosu tepla

Autor: Tobiáš Krupa

Ústav: Matematický ústav UK

Vedoucí bakalářské práce: RNDr. Ondřej Souček, Ph.D., Matematický ústav UK

Abstrakt: Tato práce je zaměřená na studium a popis úlohy přenosu tepla, při které uvažujeme také příspěvek přenosu zářením. Jde o úlohu velmi důležitou z hlediska praktického využití v průmyslu.

V úvodu práce podrobně vysvětlujeme odvození stěžejního systému řídicích rovnic pro radiační přenos tepla. Vzhledem ke komplexnosti tohoto systému pokračujeme v další části představením aproximace pomocí tzv. SP_n rovnic. Zaměříme se zejména na nejjednodušší sadu, SP_1 rovnice, které odvodíme technikou asymptotického rozvoje. Zvláštní pozornost je věnována okrajovým podmínkám Marsakova typu, které jsou v různých zdrojích formulovány nepřesně. Tyto rovnice opět asymptoticky odvodíme do správného tvaru.

Inspirováni výrobním procesem tabulového skla se zajímáme také o problematiku s více oblastmi o rozdílných indexech lomu. Pro řešení této úlohy je potřeba znát přechodové podmínky popisující chování teploty a intenzity záření na hranici mezi studovanými oblastmi. Obdobným postupem jako v případě okrajových podmínek se nám podařilo odvodit přirozenou sadu přechodových podmínek, které připouští jistou nespojitost v intenzitě záření. Tyto podmínky zřejmě doposud nebyly uvedeny v žádném článku zabývajícím se tímto tématem.

Práci zakončíme ukázkami několika numerických experimetů v softwaru *Wolfram Mathematica*, ve kterých srovnáváme naše řešení s benchmarkem dostupným v literatuře.

Klíčová slova: radiační přenos tepla, SPn aproximace, okrajové podmínky, přechodové podmínky

Contents

Introduction

In many industrial areas, it is crucial to monitor the temperature evolution of certain objects. Materials can change their properties dramatically when heated up, thus it is in our interest to be able to predict and model heat transfer in complex configurations. In the most simple setting, it suffices to simulate heat transport via conduction, but we can come across problems where this simple model is not accurate enough. Firstly, the material itself can be in motion changing form and shape, in that case, it is obvious that heat transport by convection has to be considered. Or the material could be at least semi-transparent allowing for heat to be transferred by the means of radiation. The latter case is the main subject studied in this thesis.

We take a look at the problem of heat transport between semi-transparent materials, where we assume that the energy can be transferred not only locally by conduction but is also continuously radiated in all directions. This additional assumption dramatically complicates the model structure and the governing equations as well. The heat equation is no longer a mere parabolic equation, but a complex integro-differential equation theoretically coupled with uncountably many elliptic equations.

In this thesis, we are interested in such models and techniques that make them solvable. In real-world applications, these models can describe processes like flat glass manufacturing, see attachment A for further information.

Physical summary

Now let us summarize what kind of model structure we are looking for. We are interested in the heat transfer between a stationary arrangement of several immiscible mediums, in reality, they can be for example glass, tin, and then surrounding gas, typically nitrogen. There are no heat sources, we simply let the system cool down by exchanging energy with the outer reservoir via heat conduction and thermal radiation. For such a problem, there exist a number of approaches that couple thermal evolution with various approximations to the problem of radiation transfer. Each technique brings its own challenges in the form of identification of suitable boundary and transition conditions.

Goals

This thesis is in a sense sort of follow-up on the studies of the Department of Mathematical Modeling, Charles University (Řehoř et al. [2017]) which did great analysis of mechanical models of the glass forming process described in attachment A. Their work was motivated by the needs of a company *Glass Service* and the main goal of this study is to integrate a certain approximation to the radiation heat transfer into the evolution of temperature during the cooling of glass.

Although we have this vision in the back of our minds, this thesis operates in rather general setting focusing on the derivation and analysis of the equations without committing to any actual setup or real-world data.

Outline

The thesis itself consists of four parts. In the first one we derive the full governing system of the partial differential equations that model our situation. It is achieved thanks to the tools of basic ray physics, or rather optics.

In the key second part, we look at the problem from the numerical point of view. We derive a simpler system of equations that is easier to solve and that is actually used in industrial computing. Here we talk about SP_n equations, SP_1 in particular, and we describe their idea for a specific set of assumptions.

In the third part, we test the equations with our own implementation of numerical solvers for such systems. We define chosen computing method and make some modifications to the equations resulting in them being more suitable for numerical calculations. Finally, we provide a comparison with benchmark results adopted from the literature.

The final fourth part includes a discussion about the application of the model to simple geometry setup and whether our equations are consistent. We also offer a glimpse of SP_2 equations and on how they differ from SP_1.

1. Radiative heat transfer

We begin our work with a brief overview of the subject, defining basic quantities and principles. Full analysis of the pivotal ideas regarding this matter can be found in a book written by Martin Frank and Axel Klar (Frank and Klar [2011]). It is well-known that heat can be mainly transported by three distinct mechanisms: heat conduction, material convection, and radiation. We will briefly summarize certain aspects of all of them, special attention will be then dedicated to radiation.

Heat conduction

We start with the principle of each mechanism. Conduction can be at a sufficiently fine scale described as energy transfer due to particles' interactions. These interactions are happening on an atomic length scale, 10^{-9} m (Frank and Klar [2011]). One can visualize a collision of two point-like particles, during which they exchange their energy, thus transporting it through space. According to Fourier's law, the heat flux is proportional to the local temperature difference, or rather a spatial derivative (gradient).

$$\mathbf{q}_{con} = -k\nabla T, \tag{1.1}$$

where k is *thermal conductivity* of given material. Usually, k is taken as a constant, although it doesn't have to be totally precise and in reality, it may slightly vary with temperature. However, to simplify the model, we will use constant-value approximation. Therefore in our equations, k is a constant.

Convection

This process is omitted in the models we will focus on, so we do not discuss it in detail. Convection is an energy transfer process that is directly related to the motion of the matter itself, in other words heat is carried along with the moving material. As such, the process is also local in the sense that its effectiveness depends on the local velocity and the local thermal gradient.

To illustrate this, consider a vessel full of liquid with heterogeneous temperature distribution. If there is a peak in thermal energy on one side of the vessel, by the convection and also conduction, the thermal energy has to be "passed on" through the material to reach the other side. Certain point affects only its close neighborhood.

Thermal radiation

This mechanism is not like the previous two. It is realized by travelling photons, not material particles themselves. Of course, the matter has its influence on the radiation, but it is rather inhibiting. Energy can be transferred by radiation without the need for any medium. If we again picture a situation, this time with two vessels (or simply bodies) separated with vacuum, there is no way that any energy would be transported via conduction or convection. But an exchange of

energy would still occur because of radiation. And similarly, within only one vessel (body), the hot right side immediately affects the cold left side.

As we can see, radiative transfer can be really effective. Another reason for that is so-called Stefan-Boltzmann law. It states that energy flux leaking out of volume through radiation is proportional to the **fourth power** of temperature:

$$E = \sigma T^4 \tag{1.2}$$

This means that radiation will have a significant impact when dealing with high temperatures, which is characteristic for the application we consider (see A).

We can see that thermal radiation will dramatically change the solution to the heat evolution problem. However, it is clear that we do not get by with just differential equations, since radiation is not a local process. A single point's temperature is at each moment affected by the temperature of every other point in the material. The governing system will have to contain an integral, meaning we will deal with integro-differential equations.

On the other hand, we are able to kind of get around integrating over the whole volume of the vessel, but at the cost of implementing a new unknown function that represents a direction-dependent field of radiation.

1.1 Radiative transfer equation

As we hinted above, there are several typical functions that we have to introduce first before we start deriving the radiative transfer equations (RTE). There is a wider spectrum of them actually, but we will settle with only a couple of them that are actually needed in this thesis (for further information see Frank and Klar [2011] or Howell et al. [2021], p. 4-42).

1.1.1 Physical quantities

Spectral intensity

The most important quantity in this entire work is **spectral intensity**, denoted I. It describes the radiative transport of energy at a given point $(\mathbf{x}, t)$ in space and time. It is also dependent on specific direction $\mathbf{\Omega}$ (unit vector) and lastly, on frequency ν at which the radiation propagates.

$$I(\mathbf{x}, t, \mathbf{\Omega}, \nu) \tag{1.3}$$

Its physical meaning can be stated as the amount of radiative energy dE that flows through an area dA spread into solid angle $d\mathbf{\Omega}$ over time dt in spectrum band $d\nu$. Another way of perceiving this quantity is as rays of photons traveling through a medium in a given direction at a certain energy level (frequency). This image will help us later motivate processes like absorption or scattering.

Let us emphasize here that the key feature of intensity that allows it to model complex radiative transport is the direction-dependence. It results in a quite complicated set of equations, but the complexity is naturally embedded in the problem itself. Note that we are not actually interested in knowing the shape of the intensity function. Later we will see that it will be more relevant to compute its moments, resp. directional averages.

For starters, let us define total intensity $I(\mathbf{x}, t, \mathbf{\Omega})$, as summed intensities across the whole spectrum.

$$I(\mathbf{x}, t, \mathbf{\Omega}) = \int_0^\infty I(\mathbf{x}, t, \mathbf{\Omega}, \nu)\, d\nu \tag{1.4}$$

Taking the integration one step further, we get another important quantity.

Energy flux

Next, we establish energy flux $E(\mathbf{x}, t)$, or rather $\varphi(\mathbf{x}, t)$ to be consistent with the literature. It will be essential for deriving the governing equation later because as it often goes in physics, the equation is based on energy conservation.

It is defined:

$$\varphi(\mathbf{x}, t) = \int_{S^2} I(\mathbf{x}, t, \mathbf{\Omega})\, d\mathbf{\Omega} = \int_{S^2} \int_0^\infty I(\mathbf{x}, t, \mathbf{\Omega}, \nu)\, d\nu\, d\mathbf{\Omega} \tag{1.5}$$

It will also play a key role in our diffusion-based approximation, where we employ the reduction of one of the variables, direction $\mathbf{\Omega}$. Since we are not interested in intensity after all, it does not bother us to calculate with its integrals only. We will see the point in chapter 2.

Radiative heat flux

Analogously to the conductive heat flux $\mathbf{q}$ given by Fourier's law, there is a vector quantity that describes net energy transport by means of radiation. To be consistent with the literature, let us denote it $\mathbf{F}$ and it is defined as

$$\mathbf{F}(\mathbf{x}, t) = \int_{S^2} \mathbf{\Omega} I(\mathbf{x}, t, \mathbf{\Omega})\, d\mathbf{\Omega} = \int_{S^2} \int_0^\infty \mathbf{\Omega} I(\mathbf{x}, t, \mathbf{\Omega}, \nu)\, d\nu\, d\mathbf{\Omega} \tag{1.6}$$

We could also define spectral radiative flux dependent on frequency by omitting the integral over the whole spectrum, but it will not be used in this paper anyway.

Blackbody intensity

A very important milestone in this field was Planck's distribution law. It describes the behaviour of an idealized object called a blackbody. It serves as the first approximation for any body that radiates energy.

We can visualize the energy transfer as rays of electromagnetic radiation. Any regular object is able to emit and absorb radiation within its volume and emit, absorb or reflect it at the boundary. The behavior is determined by the properties of the studied object and the energy level of the radiation. The basic relation $E = hf$ states that energy is proportionate to the frequency of the electromagnetic wave. After radiation hits an object, depending on that exact frequency, the ray is either reflected back or transferred inside.

Then, in the bulk region, the radiation can experience some sort of attenuation via absorption by individual molecules. This results in different degrees of transparency.

The blackbody approximation assumes that all the radiation that arrives at the object's surface is absorbed, ergo no radiation is reflected. Hence the name

blackbody, because due to the absence of reflection, it would appear as totally black. On top of this, the radiation emitted by this body is again through the **whole spectrum** and also **isotropic** (equal in all directions).

In this paper, we will not be spending time on deriving the formula for the blackbody intensity $B(\nu, T)$ (for details, see Frank and Klar [2011], sec. 2.2), instead we content with knowing the formula

$$B(\nu, T) = n_1^2 \frac{2h_P \nu^3}{c_0^2} \frac{1}{e^{\frac{h_P \nu}{k_B T}} - 1}, \tag{1.7}$$

where T is the thermodynamic temperature at a certain point in space and time, ν is the frequency of the radiation, n_1 is the refractive index of our environment, c_0 is the speed of light in vacuum ($c_0 = 299\,792\,458\,\mathrm{m{\cdot}s^{-1}}$), h_P is Planck constant ($h_P = 6.626 \cdot 10^{-34}\,\mathrm{J{\cdot}s}$) and k_B is Boltzmann constant ($k_B = 1.38 \cdot 10^{-23}\,\mathrm{J{\cdot}K^{-1}}$).

Note that we will also work with mediums that have different refractive indices, at those times mind the index that corresponds to the refractive index of that medium, i.e. B_1 in medium with n_1, B_2 in medium with n_2 etc. If we consider only one domain with a homogeneous medium, then we omit the index and write just B instead of B_1 to be consistent with the literature.

1.1.2 Derivation

Now that we have defined the necessary quantities, we dive deeper into relations telling how one influences the other. First, we look into the effects on intensity in bulk regions.

Absorption

As we stated earlier, the radiation propagating through a medium is slowly and partially reduced due to a number of phenomena, absorption being one of them. This process can be explained by the image of photons colliding with atoms, getting absorbed, and exciting them onto higher energy levels, thus the radiation itself loses energy. The number of encountered atoms is clearly linearly dependent on the traveled distance Δs. We simplify the situation by introducing a single parameter κ that describes the absorbing properties of the material. It tells us the proportion of energy that is passed on from photons to atoms. If we now imagine a ray of photons that travel distance Δs through a medium, we can state simple relation for the decrease of intensity:

$$I(\mathbf{x} + \boldsymbol{\Omega}\Delta s, t + \frac{\Delta s}{c}, \boldsymbol{\Omega}, \nu) = I(\mathbf{x}, t, \boldsymbol{\Omega}, \nu) - \kappa I(\mathbf{x}, t, \boldsymbol{\Omega}, \nu)\Delta s \tag{1.8}$$

where c is the speed of light in considered medium ($c = \frac{c_0}{n_1}$).

Emission

On the other hand, there are also sources that increase the intensity, here we exclusively mean the thermal radiating of the medium. Although thermal radiation is mainly related to higher temperatures, it is (just like gravity force) constantly happening even at the scale of everyday objects at room temperature (as long as

the temperature is not 0). Therefore, if we study the intensity field in a body we do not get by with considering only incoming outer radiation that decays inside. The overall field of intensity will be also magnified by inner radiation.

This emitted radiation will be referred to as emission and its intensity is in the form of isotropic blackbody intensity. If we again keep track of intensity as we move through the medium, the contribution of emission is linearly dependent on that traveled distance (number of atoms come across). For the intensity balance, we can set up a similar relation:

$$I(\mathbf{x} + \mathbf{\Omega}\Delta s, t + \frac{\Delta s}{c}, \mathbf{\Omega}, \nu) = I(\mathbf{x}, t, \mathbf{\Omega}, \nu) + \kappa B(\nu, T)\Delta s \tag{1.9}$$

We can see that we used the same constant κ as in the equation (1.8). We can validate this step by considering a blackbody-like material. If the absorption was different from emission, there would spontaneously arise a magnifying intensity field.

Scattering

For the sake of completeness, we have to mention also the process of scattering, as it can also alter the intensity field. The key observation is that the intensity $I(\mathbf{x}, t, \mathbf{\Omega}, \nu)$ is direction-dependent and scattering is the process during which the radiation is sort of randomly distributed into other directions. We recall the image of a photon traveling in direction $\mathbf{\Omega}'$ colliding with atom. If it is not absorbed, it is instead redirected to other direction $\mathbf{\Omega}$. Or in other words, photons from various directions $\mathbf{\Omega}'$ can be directed in $\mathbf{\Omega}$, the direction of interest (now the notation makes more sense).

The "random" character of scattering is modeled by probability density function $s(\mathbf{\Omega}, \mathbf{\Omega}')$ that determines the probability of change of direction $\mathbf{\Omega}' \longrightarrow \mathbf{\Omega}$. Since it represents the probability, it has to hold that:

$$\int_{S^2} s(\mathbf{\Omega}, \mathbf{\Omega}')\, d\mathbf{\Omega}' = 1 \tag{1.10}$$

where we integrate over unit sphere S^2.

We again assert that the amount of scattered radiation is proportional to the distance traveled by the ray of photons, let us denote the constant of proportionality by σ.

Similarly to the absorption/emission balance, we have the term contributing to increase of the intensity in our direction $\mathbf{\Omega}$, so called in-scattering term, as well as the term representing the decrease, out-scattering term.

$$\begin{aligned} &I(\mathbf{x} + \mathbf{\Omega}\Delta s, t + \frac{\Delta s}{c}, \mathbf{\Omega}, \nu) = \\ &\quad = I(\mathbf{x}, t, \mathbf{\Omega}, \nu) + \sigma \left(\int_{S^2} s(\mathbf{\Omega}, \mathbf{\Omega}') I(\mathbf{x}, t, \mathbf{\Omega}', \nu)\, d\mathbf{\Omega}' - I(\mathbf{x}, t, \mathbf{\Omega}, \nu) \right) \Delta s \end{aligned} \tag{1.11}$$

The integral in equation (1.11) accounts for all possible directions on S^2 from which the radiation might be reflected. The out-scattering term $-\sigma I \Delta s$ is analogous to absorption or emission terms.

One thing we may be interested in is the actual form of the function $s(\mathbf{\Omega}, \mathbf{\Omega}')$. It turns out that isometric approximation is fairly accurate and, of course, it

simplifies the model. We will therefore in this paper consider $s(\mathbf{\Omega}, \mathbf{\Omega}') \equiv \frac{1}{4\pi}$. Later, we will point out the step of derivation at which this assumption makes the scattering effect vanish from the equations.

Now we consider all the previous effects (equations (1.8), (1.9) and (1.11)) acting at the same time and we get a balance equation for intensity $I(\mathbf{x}, t, \mathbf{\Omega}, \nu)$:

$$I(\mathbf{x} + \mathbf{\Omega}\Delta s, t + \frac{\Delta s}{c}, \mathbf{\Omega}, \nu) = I(\mathbf{x}, t, \mathbf{\Omega}, \nu) + \Big[\kappa\Big(B(\nu, T) - I(\mathbf{x}, t, \mathbf{\Omega}, \nu)\Big) + \\ + \sigma\left(\int_{S^2} s(\mathbf{\Omega}, \mathbf{\Omega}') I(\mathbf{x}, t, \mathbf{\Omega}', \nu)\, d\mathbf{\Omega}' - I(\mathbf{x}, t, \mathbf{\Omega}, \nu)\right)\Big] \Delta s \quad (1.12)$$

We will gather the terms of the difference quotient on the left-hand side

$$\frac{I(\mathbf{x} + \mathbf{\Omega}\Delta s, t + \frac{\Delta s}{c}, \mathbf{\Omega}, \nu) - I(\mathbf{x}, t, \mathbf{\Omega}, \nu)}{\Delta s} = \kappa\Big(B(\nu, T) - I(\mathbf{x}, t, \mathbf{\Omega}, \nu)\Big) + \\ + \sigma\left(\int_{S^2} s(\mathbf{\Omega}, \mathbf{\Omega}') I(\mathbf{x}, t, \mathbf{\Omega}', \nu)\, d\mathbf{\Omega}' - I(\mathbf{x}, t, \mathbf{\Omega}, \nu)\right) \quad (1.13)$$

and take the limit $\Delta s \longrightarrow 0$,

Full Radiative transfer equation

$$\mathbf{\Omega} \cdot \nabla I(\mathbf{x}, t, \mathbf{\Omega}, \nu) + \frac{1}{c}\frac{\partial}{\partial t} I(\mathbf{x}, t, \mathbf{\Omega}, \nu) = \kappa\Big(B(\nu, T) - I(\mathbf{x}, t, \mathbf{\Omega}, \nu)\Big) + \\ + \sigma\left(\int_{S^2} s(\mathbf{\Omega}, \mathbf{\Omega}') I(\mathbf{x}, t, \mathbf{\Omega}', \nu)\, d\mathbf{\Omega}' - I(\mathbf{x}, t, \mathbf{\Omega}, \nu)\right). \quad (1.14)$$

Thus we got the **Radiative transfer equation** in its full form.

As we have hinted before, some terms will not play a significant role in further derivation. Firstly, it is the scattering term which we assume to be isometric and secondly, it's the term with time derivative. The time that radiation needs to propagate through a medium is much smaller than the considered time scale. So, we neglect any momentary changes and treat the intensity at any time as in its stationary state. We can also naively motivate this step by saying that the coefficient $\frac{1}{c}$ in front of that term is very small. After this reasoning, we get a steady radiative transfer equation:

$$\mathbf{\Omega} \cdot \nabla I(\mathbf{x}, t, \mathbf{\Omega}, \nu) = \kappa\Big(B(\nu, T) - I(\mathbf{x}, t, \mathbf{\Omega}, \nu)\Big) + \\ + \sigma\left(\int_{S^2} s(\mathbf{\Omega}, \mathbf{\Omega}') I(\mathbf{x}, t, \mathbf{\Omega}', \nu)\, d\mathbf{\Omega}' - I(\mathbf{x}, t, \mathbf{\Omega}, \nu)\right) \quad (1.15)$$

from which we later deduce the heat flux for the energy balance equation.

1.2 Energy conservation

In this section, we will finally discuss equations concerning temperature T, our desired quantity. We directly focus on the equation representing the conservation

of energy of incompressible fluid (we have adopted the formula from lecture notes Matyska [2005]).

$$\rho_m c_m \frac{\partial T}{\partial t} = -\rho_m c_m \mathbf{v} \cdot \nabla T - \nabla \cdot \mathbf{q} + aT \left(\frac{\partial p}{\partial t} + \mathbf{v} \cdot \nabla p \right) + \mathbf{t}^D : \nabla \mathbf{v} + \rho_m h_m \tag{1.16}$$

where ρ_m is the density of the medium, c_m is its heat capacity, $\mathbf{v}$ is the velocity vector, $\mathbf{q}$ is the heat flux, a is thermal expansion coefficient, p is pressure, $\mathbf{t}$ is the Cauchy stress tensor and h_m represents inner sources of heat. There are quite a lot of complicated terms, however, most of them vanish because we consider our medium at rest, ergo $\mathbf{v} = 0$. Plus, we do not consider any heat generated inside our medium, $h_m = 0$.

These assumptions greatly simplify the equation into the form:

$$\rho_m c_m \frac{\partial T}{\partial t} = -\nabla \cdot \mathbf{q} \tag{1.17}$$

One may think that we reduced the problem to a simple heat equation, but keep in mind that $\mathbf{q}$ does not represent mere conduction, it includes radiative heat transport.

$$\mathbf{q} = \mathbf{q}_{con} + \mathbf{F} \tag{1.18}$$

For $\mathbf{q}_{con}$ we can simply substitute from equation (1.1) and get:

$$-\nabla \cdot \mathbf{q}_{con} = \nabla \cdot (k \nabla T) \tag{1.19}$$

We can rewrite $\mathbf{F}$ according to our definition (1.6):

$$-\nabla \cdot \mathbf{F}(\mathbf{x}, t) = -\nabla \cdot \int_{S^2} \int_0^\infty \mathbf{\Omega} I(\mathbf{x}, t, \mathbf{\Omega}, \nu) \, d\nu \, d\mathbf{\Omega} \tag{1.20}$$

Now we interchange differentiation and integration as they are independent and then we use the relation from steady radiative transfer equation (1.15).

$$\begin{aligned} -\nabla \cdot \mathbf{F}(\mathbf{x}, t) &= -\int_{S^2} \int_0^\infty \mathbf{\Omega} \cdot \nabla I(\mathbf{x}, t, \mathbf{\Omega}, \nu) \, d\nu \, d\mathbf{\Omega} \\ &= -\int_{S^2} \int_0^\infty \kappa \Big(B(\nu, T) - I(\mathbf{x}, t, \mathbf{\Omega}, \nu) \Big) \, d\nu \, d\mathbf{\Omega} + \\ &\quad + \int_{S^2} \int_0^\infty \sigma \left(\int_{S^2} s(\mathbf{\Omega}, \mathbf{\Omega}') I(\mathbf{x}, t, \mathbf{\Omega}', \nu) \, d\mathbf{\Omega}' - I(\mathbf{x}, t, \mathbf{\Omega}, \nu) \right) \, d\nu \, d\mathbf{\Omega} \end{aligned} \tag{1.21}$$

We will take a closer look on that second integral term and recall the assumption of isotropic radiation scattering:

$$\begin{aligned} &\int_{S^2} \int_0^\infty \sigma \left(\int_{S^2} s(\mathbf{\Omega}, \mathbf{\Omega}') I(\mathbf{x}, t, \mathbf{\Omega}', \nu) \, d\mathbf{\Omega}' - I(\mathbf{x}, t, \mathbf{\Omega}, \nu) \right) \, d\nu \, d\mathbf{\Omega} = \\ &\quad = \int_{S^2} \sigma \left(\int_{S^2} s(\mathbf{\Omega}, \mathbf{\Omega}') I(\mathbf{x}, t, \mathbf{\Omega}') \, d\mathbf{\Omega}' - I(\mathbf{x}, t, \mathbf{\Omega}) \right) \, d\mathbf{\Omega} = \\ &\quad = \sigma \int_{S^2} \int_{S^2} \frac{1}{4\pi} I(\mathbf{x}, t, \mathbf{\Omega}') \, d\mathbf{\Omega}' \, d\mathbf{\Omega} - \sigma \int_{S^2} I(\mathbf{x}, t, \mathbf{\Omega}) \, d\mathbf{\Omega} = \\ &\quad = \sigma \left(\frac{1}{4\pi} \int_{S^2} I(\mathbf{x}, t, \mathbf{\Omega}') \, d\mathbf{\Omega}' \cdot \int_{S^2} d\mathbf{\Omega} - \int_{S^2} I(\mathbf{x}, t, \mathbf{\Omega}) \, d\mathbf{\Omega} \right) = \\ &\quad = \sigma \left(\int_{S^2} I(\mathbf{x}, t, \mathbf{\Omega}') \, d\mathbf{\Omega}' - \int_{S^2} I(\mathbf{x}, t, \mathbf{\Omega}) \, d\mathbf{\Omega} \right) = 0 \end{aligned} \tag{1.22}$$

At this point we see that for isotropic scattering, the in and out scattering terms cancel out, this is what we have insinuated earlier. Therefore substituting everything back will give us the final form of governing bulk equation for temperature.

Temperature evolutionary equation

$$\rho_m c_m \frac{\partial T(\mathbf{x},t)}{\partial t} = \nabla \cdot (k \nabla T(\mathbf{x},t)) - \int_0^\infty \int_{S^2} \kappa \Big(B(\nu,T) - I(\mathbf{x},t,\mathbf{\Omega},\nu) \Big) \, d\mathbf{\Omega} \, d\nu \tag{1.23}$$

1.3 Boundary conditions

So far, we have obtained two time-dependent partial integro-differential equations, (1.15) and (1.23), for unknown functions $I(\mathbf{x},t,\mathbf{\Omega},\nu)$ and $T(\mathbf{x},t)$. Naturally, there is a question of initial and boundary conditions present. First, we look at the boundary condition for intensity I. In this section we still follow the work of Frank and Klar (Frank and Klar [2011]).

1.3.1 Intensity boundary condition

As an electromagnetic ray hits an object's boundary, one of two things must happen. Either it is reflected according to *law of reflection* back into the same material, or it is transmitted through to the other material behind the boundary.

We consider a flat (for simplicity) boundary between two mediums, $\mathcal{M}_1$ and $\mathcal{M}_2$, and radiation passing through it, see figure 1.1. Their refractive indices are n_1 and n_2, respectively. We can assume that $n_1 > n_2$ because in the real case, our goal is to model a glass panel ($\mathcal{M}_1$) surrounded by air or other gas ($\mathcal{M}_2$). We would like to determine intensity at boundary point $\mathbf{x} \in \partial\mathcal{M}_1$ in direction $\mathbf{\Omega}$ aiming into medium $\mathcal{M}_1$.

Reflectivity

First, let us establish the basic notation. As we know the ray of electromagnetic radiation changes on crossing the boundary its direction. This change is described by *Snell's law*:

$$n_1 \sin(\theta_1) = n_2 \sin(\theta_2) \tag{1.24}$$

where θ_1 and θ_2 are the angles at which do directions of the ray meet with the normal line passing through $\mathbf{x}$ in $\mathcal{M}_1$ and $\mathcal{M}_2$ resp. Let us then denote $\mathbf{n}$ a unit normal vector at point $\mathbf{x}$ pointing into $\mathcal{M}_2$ ($\mathbf{n} \cdot \mathbf{\Omega} < 0$) and $\mathbf{\Omega}_i$ (for *incident*) the direction that gets transformed on the boundary into $\mathbf{\Omega}$. Then $\cos(\theta_1) = \cos(\theta) = |\mathbf{n} \cdot \mathbf{\Omega}|$ and $\cos(\theta_2) = \cos(\theta_i) = |\mathbf{n} \cdot \mathbf{\Omega}_i|$.

Naturally, not all the radiation hitting a boundary gets transmitted to the other side. Transmittance of a boundary can be for simplicity characterized by a single parameter: reflectivity ρ. It represents the ratio between the number of photons which are reflected and the total amount that hit the boundary. It

generally depends on the angle of incidence, particularly on the quantity $|\mathbf{n}\cdot\boldsymbol{\Omega}|$ since we care about the slant of $\boldsymbol{\Omega}$ instead of its orientation.

However, what really does matter, is on which side of the boundary we consider the reflection happening. For example, above the critical angle θ_c, the reflectivity on one side will be equal to 1, while the same does not apply to the other side. It can also be shown directly from the formula for $\rho(|\mathbf{n}\cdot\boldsymbol{\Omega}|)$ itself. We, therefore, have to distinguish between reflectivity ρ_1 that describes the behavior of a ray coming to the boundary from medium $\mathcal{M}_1$ and analogous reflectivity ρ_2 in $\mathcal{M}_2$. For each one, we are able to put together an explicit formula, a. k. as Fresnel equation (Howell et al. [2021], p. 90) ($\mu = |\mathbf{n}\cdot\boldsymbol{\Omega}| = \cos\theta_1$ in equation (1.25) or $\mu = |\mathbf{n}\cdot\boldsymbol{\Omega}_i| = \cos\theta_2$ in (1.26)):

$$\rho_1(\mu) = \begin{cases} 1 & ,\mu \leq \sqrt{1-\left(\frac{n_2}{n_1}\right)^2} \\ \frac{1}{2}\left[\left|\frac{n_1\mu - n_2\sqrt{1-\left(\frac{n_1}{n_2}\right)^2(1-\mu^2)}}{n_1\mu + n_2\sqrt{1-\left(\frac{n_1}{n_2}\right)^2(1-\mu^2)}}\right|^2 + \left|\frac{n_1\sqrt{1-\left(\frac{n_1}{n_2}\right)^2(1-\mu^2)} - n_2\mu}{n_1\sqrt{1-\left(\frac{n_1}{n_2}\right)^2(1-\mu^2)} + n_2\mu}\right|^2\right] & ,\mu > \sqrt{1-\left(\frac{n_2}{n_1}\right)^2} \end{cases} \tag{1.25}$$

$$\rho_2(\mu) = \frac{1}{2}\left[\left|\frac{n_2\mu - n_1\sqrt{1-\left(\frac{n_2}{n_1}\right)^2(1-\mu^2)}}{n_2\mu + n_1\sqrt{1-\left(\frac{n_2}{n_1}\right)^2(1-\mu^2)}}\right|^2 + \left|\frac{n_2\sqrt{1-\left(\frac{n_2}{n_1}\right)^2(1-\mu^2)} - n_1\mu}{n_2\sqrt{1-\left(\frac{n_2}{n_1}\right)^2(1-\mu^2)} + n_1\mu}\right|^2\right] \tag{1.26}$$

The formula for intensity at boundary point $\mathbf{x}$ in direction $\boldsymbol{\Omega}$ aiming into medium $\mathcal{M}_1$ reads:

$$I(\mathbf{x}, t, \boldsymbol{\Omega}, \nu) = I_{ref} + I_{tr} \tag{1.27}$$

It means that the intensity at the boundary is solely merged from two separate components.

First is the intensity I_{ref} originally heading out into medium $\mathcal{M}_2$ but reflected back. The initial direction can be easily deduced from the law of reflection. If the final direction of our intensity is $\boldsymbol{\Omega}$, then the initial direction has to be

$$\boldsymbol{\Omega}' = \boldsymbol{\Omega} - 2(\mathbf{n}\cdot\boldsymbol{\Omega})\mathbf{n} \tag{1.28}$$

Of course, the reflected intensity is only a portion of $I(\mathbf{x}, t, \boldsymbol{\Omega}', \nu)$ as part of it is transmitted into $\mathcal{M}_2$. The ratio is given by aforementioned reflectivity $\rho_1(|\mathbf{n}\cdot\boldsymbol{\Omega}'|) \in [0, 1]$

$$I_{ref} = \rho_1(|\mathbf{n}\cdot\boldsymbol{\Omega}'|)I(\mathbf{x}, t, \boldsymbol{\Omega}'\nu) \tag{1.29}$$

The second term, I_{tr} is a bit trickier. It represents the contribution of intensity that is transmitted through the boundary from $\mathcal{M}_2$. Here we deal with radiation

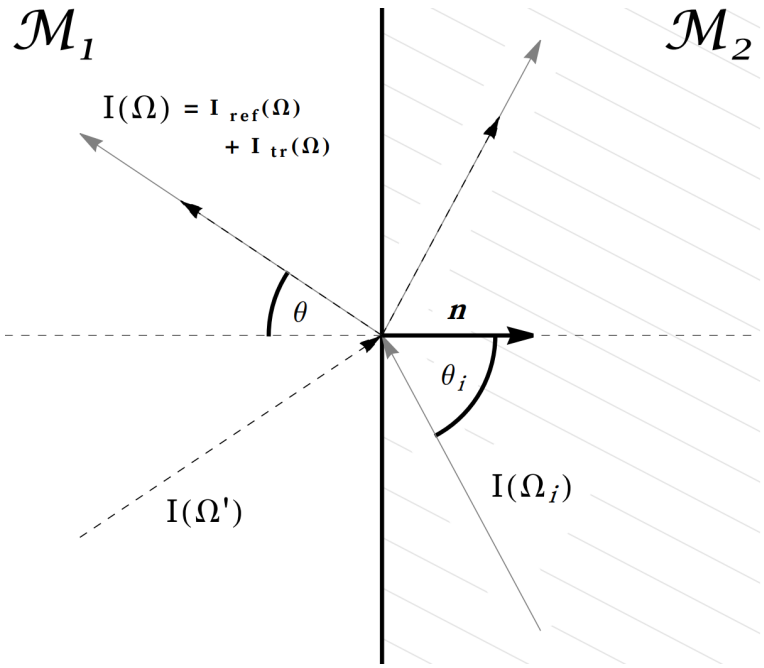

Figure 1.1: Boundary between mediums $\mathcal{M}_1$ and $\mathcal{M}_2$

that comes over from the environment with a different refractive index, hence $\mathbf{\Omega}_i \neq \mathbf{\Omega}$. However, the direction is not the only parameter that changes. If we take a look at the bundle of rays in solid angle $d\mathbf{\Omega}_i$ when passing through the boundary from $\mathcal{M}_2$ into $\mathcal{M}_1$, they all change direction as expected, but the resulting cone narrows down, in other words, the solid angle gets smaller. This phenomenon is well described in (Howell et al. [2021], p. 836-838) Rigorously we can describe this shrinkage as follows:

$$\begin{aligned} \sin(\theta_2) &= \frac{n_1}{n_2}\sin(\theta_1) \\ \cos(\theta_2)\,d\theta_2 &= \frac{n_1}{n_2}\cos(\theta_1)\,d\theta_1 \\ \cos(\theta_2)\,d\mathbf{\Omega}_i = \cos(\theta_2)\sin(\theta_2)\,d\theta_2\,d\phi &= \left(\frac{n_1}{n_2}\right)^2 \cos(\theta_1)\sin(\theta_1)\,d\theta_1\,d\phi = \left(\frac{n_1}{n_2}\right)^2 \cos(\theta_1)\,d\mathbf{\Omega} \end{aligned} \tag{1.30}$$

Once again, we use the conservation of energy which we express from definition of intensity.

$$dE_1 = I_{tr}(\mathbf{x}, t, \mathbf{\Omega}, \nu)\,dA_1\,d\mathbf{\Omega}\,dt\,d\nu \tag{1.31}$$

$$dE_2 = [1 - \rho_2(|\mathbf{n}\cdot\mathbf{\Omega}_i|)]\,I(\mathbf{x}, t, \mathbf{\Omega}_i, \nu)\,dA_2\,d\mathbf{\Omega}_i\,dt\,d\nu \tag{1.32}$$

Note that the area dA_1, resp. dA_2, is meant in plane perpendicular to $\mathbf{\Omega}$, resp. $\mathbf{\Omega}_i$. If we consider infinitesimal area dA in the boundary plane at point $\mathbf{x}$, it

holds $dA_1 = \cos\theta_1\, dA,\ dA_2 = \cos\theta_2\, dA$. Energy must be conserved, hence:

$$\begin{aligned} dE_1 &= dE_2 \\ I_{tr}(\mathbf{x},t,\mathbf{\Omega},\nu)\, dA_1\, d\mathbf{\Omega}\, dt\, d\nu &= [1-\rho_2(|\mathbf{n}\cdot\mathbf{\Omega}_i|)]\, I(\mathbf{x},t,\mathbf{\Omega}_i,\nu)\, dA_2\, d\mathbf{\Omega}_i\, dt\, d\nu \\ I_{tr}(\mathbf{x},t,\mathbf{\Omega},\nu)\cos(\theta_1)\, dA\, d\mathbf{\Omega}\, dt\, d\nu &= \\ & [1-\rho_2(|\mathbf{n}\cdot\mathbf{\Omega}_i|)] I(\mathbf{x},t,\mathbf{\Omega}_i,\nu)\cos(\theta_2)\, dA\, d\mathbf{\Omega}_i\, dt\, d\nu \\ I_{tr}(\mathbf{x},t,\mathbf{\Omega},\nu)\cos(\theta_1)\, dA\, d\mathbf{\Omega}\, dt\, d\nu &= \\ & [1-\rho_2(|\mathbf{n}\cdot\mathbf{\Omega}_i|)] I(\mathbf{x},t,\mathbf{\Omega}_i,\nu)\left(\frac{n_1}{n_2}\right)^2\cos(\theta_1)\, dA\, d\mathbf{\Omega}\, dt\, d\nu \end{aligned} \tag{1.33}$$

From this, it follows that:

$$I_{tr}(\mathbf{x},t,\mathbf{\Omega},\nu) = [1-\rho_2(|\mathbf{n}\cdot\mathbf{\Omega}_i|)]\left(\frac{n_1}{n_2}\right)^2 I(\mathbf{x},t,\mathbf{\Omega}_i,\nu) \tag{1.34}$$

Putting together formulas (1.27), (1.29), and (1.34) we obtain the final form of the boundary condition for intensity.

Boundary condition to (RTE)

$$I(\mathbf{x},t,\mathbf{\Omega},\nu) = \rho_1(|\mathbf{n}\cdot\mathbf{\Omega}'|)I(\mathbf{x},t,\mathbf{\Omega}'\nu) + [1-\rho_2(|\mathbf{n}\cdot\mathbf{\Omega}_i|)]\left(\frac{n_1}{n_2}\right)^2 I(\mathbf{x},t,\mathbf{\Omega}_i,\nu) \tag{1.35}$$

1.3.2 Temperature boundary condition

We try to come up with suitable boundary conditions for our modified heat equation (1.23). We consider a region of interest containing medium $\mathcal{M}_1$ in which we calculate the evolution of temperature T. Let it be surrounded by medium $\mathcal{M}_2$ with its own temperature T_2. We are not interested in fixing the temperature T at a constant value at the boundary, rather we want to model the heat flux that flows through the boundary. We do that using a parameterization of heat transfer across thin layers, standard in engineering:

$$k(\mathbf{n}\cdot\nabla)T(\mathbf{x},t) = h\,(T_2(\mathbf{x},t) - T(\mathbf{x},t)) \tag{1.36}$$

where h is a parameter describing the boundary properties and is determined by experiment.

The next remark is quite important and has a significant impact on the discussed problem. It turns out naturally that glass does not allow radiation to propagate across the whole spectrum. Below a certain threshold, a frequency ν_1, the material starts acting like blackbody material, $I \equiv B$. We call this part of the spectrum the *opaque band*. The behavior of intensity in the opaque band has a significant impact on bulk equations. Firstly, the equation (1.15) does not make sense in the opaque band since it has been posed for direction-dependent intensity field instead of isotropic intensity B. And in equation (1.23), the integrand on the right-hand side vanishes for all frequencies $\nu < \nu_1$.

The last note is about intensity boundary condition in the opaque band. It is clear that the behaviour is not the same as described in the previous section. For

example, at the boundary of a blackbody object, there is no reflection of incoming radiation, everything is absorbed. So, instead of complex intensity combining, the material simply radiates energy in the form of blackbody intensity corresponding to its temperature T and absorbs incoming blackbody radiation at surrounding temperature T_2, with no reflectivities involved. Since all this radiation is coming from and going to medium $\mathcal{M}_2$, it is in the form of B_2 (mind the index). We can consider the resulting heat flux and include this phenomenon in the temperature boundary condition.

We need to calculate the normal component of the heat flux which is fairly straightforward since $B_2(\nu, T)$ does not depend on $\mathbf{\Omega}$.

$$\begin{aligned}\mathbf{n}\cdot\mathbf{F}_{out}(\mathbf{x},t) &= \int_0^{\nu_1}\int_{H^2}\mathbf{n}\cdot\mathbf{\Omega}B_2(\nu,T)\,d\mathbf{\Omega}\,d\nu = \int_{H^2}\mathbf{n}\cdot\mathbf{\Omega}\,d\mathbf{\Omega}\int_0^{\nu_1}B_2(\nu,T)\,d\nu = \\ &= \int_{H^2}\cos(\theta)\sin(\theta)\,d\theta\,d\phi\int_0^{\nu_1}B_2(\nu,T)\,d\nu = \pi\int_0^{\nu_1}B_2(\nu,T)\,d\nu\end{aligned} \tag{1.37}$$

H^2 denotes the hemisphere with rotational symmetry around the vector $\mathbf{n}$. $\mathbf{F}_{in}$ is calculated in a similar way and after calibrations needed due to refractive indexes n_1 and n_2, we obtain full boundary condition for temperature.

$$k(\mathbf{n}\cdot\nabla)T(\mathbf{x},t) = h\left(T_2(\mathbf{x},t) - T(\mathbf{x},t)\right) + \alpha\pi\int_0^{\nu_1}B_2(\nu,T_2) - B_2(\nu,T)\,d\nu \tag{1.38}$$

We have not fully derived this formula, we only hinted possible way, the rest is adopted from (Frank and Klar [2011]). Here, α is so-called hemispheric emissivity and it is defined as

$$\alpha = 2n_1\int_0^1 1-\rho_1(\mu)\,d\mu \tag{1.39}$$

1.4 Governing system

Now let us summarize our development in the derivation. We have derived two bulk equations, the radiative transfer equation (1.15) and heat equation (1.23). And together with that, for each unknown function we have also obtained equation that describes its behaviour on the boundary. Let us rewrite this system for specific setup. Consider a volume of medium $\mathcal{M}_1$ with refractive index n_1 surrounded by medium $\mathcal{M}_2$, which is a thermal reservoir. The outer radiation coming from $\mathcal{M}_2$ to $\mathcal{M}_1$ is Planckian in distribution. To emphasize the difference between the nature of domain $\mathcal{M}_1$ and reservoir $\mathcal{M}_2$, at the end of this section we denote quantities associated with the reservoir by lower index b (blackbody-like). $\mathcal{M}_2$, or rather later $\mathcal{M}_b$, has refractive index $n_2 = n_b$ and $\rho_2 = \rho_b$. We assume that $\mathcal{M}_b$ is at constant temperature $T_2 = T_b$. Intensity B_2 gets redenoted too, in fact we start denoting $B_2 = B_b$ and $T_2 = T_b$ immediately from now on, just to keep reminding us that they are associated with blackbody-like reservoir.

Full radiative transfer equations (RTE)

$$\rho_m c_m \frac{\partial T(\mathbf{x},t)}{\partial t} = \nabla \cdot (k \nabla T(\mathbf{x},t)) - \int_{\nu_1}^{\infty} \int_{S^2} \kappa \Big(B(\nu,T) - I(\mathbf{x},t,\mathbf{\Omega},\nu) \Big) \, d\mathbf{\Omega} \, d\nu \tag{1.40a}$$

$$\begin{aligned} \mathbf{\Omega} \cdot \nabla I(\mathbf{x},t,\mathbf{\Omega},\nu) =& \kappa \Big(B(\nu,T) - I(\mathbf{x},t,\mathbf{\Omega},\nu) \Big) + \\ &+ \sigma \left(\int_{S^2} s(\mathbf{\Omega},\mathbf{\Omega}') I(\mathbf{x},t,\mathbf{\Omega}',\nu) \, d\mathbf{\Omega}' - I(\mathbf{x},t,\mathbf{\Omega},\nu) \right) \end{aligned} \tag{1.40b}$$

for all inner points $\mathbf{x} \in \mathcal{M}_1$.

Boundary condition to (RTE)

$$k(\mathbf{n} \cdot \nabla) T(\mathbf{x},t) = h \left(T_b - T(\mathbf{x},t) \right) + \alpha \pi \int_0^{\nu_1} B_b(\nu, T_b) - B_b(\nu, T) \, d\nu \tag{1.41a}$$

$$I(\mathbf{x},t,\mathbf{\Omega},\nu) = \rho_1(|\mathbf{n} \cdot \mathbf{\Omega}'|) I(\mathbf{x},t,\mathbf{\Omega}'\nu) + \left[1 - \rho_2(|\mathbf{n} \cdot \mathbf{\Omega}_i|) \right] \left(\frac{n_1}{n_b} \right)^2 B_b(\nu, T_b) \tag{1.41b}$$

for all points at the boundary $\partial \mathcal{M}_1$. Since the equation (1.40a) is evolutionary, it has to be accompanied with initial condition

$$T_0(\mathbf{x}) := T(\mathbf{x}, 0). \tag{1.42}$$

Note that in equation (1.40b) we allow only for frequencies $\nu > \nu_1$.

This system accurately captures the temperature evolution as the energy is partially transported via radiation. However, even though we have made some strong simplifying assumptions during the derivation, it is still incredibly difficult system of equations to solve.

The main cause of difficulties has proved to be the directional dependence of the intensity function and the integral coupling. It makes the system in essence contain continuous set of functions for each direction separately, and only then coupled in the equation (1.40a). Not to mention similar problem with frequency spectrum. We have to therefore further simplify our model and try to obtain reasonable equations. We will achieve this by diffusive approximation for the intensity field.

2. SP_n approximation

In this section, we assemble a simpler system of equations that is actually used in industrial computing, the methods used for derivation are adopted from article written by Edward W. Larsen et al. (Larsen et al. [2002]). These approximations yield so-called SP_n equations, simplified P_n equations. In spite of their name, the connection between SP_n and P_n equations is somewhat vague and indirect. In this paper, we avoid the formulation of P_n equations altogether and derive our system of SP_n equations completely independently of them.

The idea is to consider an optically thick medium with a great absorption coefficient κ. In this environment, it is not absurd to assume that the radiation is propagating in a diffusion-like manner, rather than via an elaborate (ray-type) transport process. We therefore aim at obtaining a diffusion equation that would reasonably describe the behavior for all directions at once.

Our approach in deriving SP_n equations is based on an asymptotic approximation as described for example in (Larsen et al. [2002]). Another known procedure is by variational analysis (Brantley and Larsen [2000]), but it turns out to be more formal and less illustrative.

We start with reformulating the governing equations into a dimensionless form that allows us to rigorously neglect small terms. We establish two referential scaling relations

$$t_{ref} = c_m \rho_m \kappa_{ref} x_{ref}^2 \frac{T_{ref}}{I_{ref}} \qquad\qquad k_{ref} = \frac{I_{ref}}{\kappa_{ref} T_{ref}} \tag{2.1}$$

according to (Larsen et al. [2002]). If we then denote

$$\varepsilon = \frac{1}{\kappa_{ref} x_{ref}} \tag{2.2}$$

we get dimensionless parameter ε which can be used to rewrite equations (1.40a), (1.40b), (1.41a) and (1.41b) like this:

$$\varepsilon^2 \frac{\partial T(\mathbf{x},t)}{\partial t} = \varepsilon^2 \nabla \cdot (k \nabla T(\mathbf{x},t)) - \int_{\nu_1}^{\infty} \int_{S^2} \kappa \Big(B(\nu,T) - I(\mathbf{x},t,\mathbf{\Omega},\nu) \Big)\, d\mathbf{\Omega}\, d\nu \tag{2.3a}$$

$$\varepsilon \mathbf{\Omega} \cdot \nabla I(\mathbf{x},t,\mathbf{\Omega},\nu) = \kappa \Big(B(\nu,T) - I(\mathbf{x},t,\mathbf{\Omega},\nu) \Big) \tag{2.3b}$$

for all inner points $\mathbf{x} \in \mathcal{M}_1$ and

$$\varepsilon k (\mathbf{n} \cdot \nabla) T(\mathbf{x},t) = h\,(T_b - T(\mathbf{x},t)) + \alpha\pi \int_0^{\nu_1} B_b(\nu,T_b) - B_b(\nu,T)\, d\nu \tag{2.4a}$$

$$I(\mathbf{x},t,\mathbf{\Omega},\nu) = \rho_1(|\mathbf{n} \cdot \mathbf{\Omega}'|) I(\mathbf{x},t,\mathbf{\Omega}'\nu) + [1 - \rho_2(|\mathbf{n} \cdot \mathbf{\Omega}_i|)] \left(\frac{n_1}{n_2}\right)^2 B_b(\nu,T_b) \tag{2.4b}$$

for points on the boundary $\partial\mathcal{M}_1$.

Note that we have again neglected the scattering effect, we plan on integrating over a sphere so it would vanish anyway, see (1.22). Let us proceed with the derivation itself.

2.1 SP_1 model derivation

We start with our derivation by rewriting equation (2.3b) in a special form.

$$\left(1+\frac{\varepsilon}{\kappa}\boldsymbol{\Omega}\cdot\nabla\right)I(\mathbf{x},t,\boldsymbol{\Omega},\nu)=B(\nu,T) \tag{2.5}$$

Now we invert the operator via a mathematical trick, known as the Neumann series for operators (Larsen et al. [2002]). Let us note that the whole procedure of deriving the $\mathrm{SP_n}$ equations asymptotically is only formal and we do not examine its mathematical correctness.

$$\begin{aligned}
I(\mathbf{x},t,\boldsymbol{\Omega},\nu)&=\left(1+\frac{\varepsilon}{\kappa}\boldsymbol{\Omega}\cdot\nabla\right)^{-1}B(\nu,T)\\
I(\mathbf{x},t,\boldsymbol{\Omega},\nu)&=\left[1+\left(-\frac{\varepsilon}{\kappa}\boldsymbol{\Omega}\cdot\nabla\right)+\left(-\frac{\varepsilon}{\kappa}\boldsymbol{\Omega}\cdot\nabla\right)^2+\left(-\frac{\varepsilon}{\kappa}\boldsymbol{\Omega}\cdot\nabla\right)^3+\ldots\right]B(\nu,T)\\
I(\mathbf{x},t,\boldsymbol{\Omega},\nu)&=\left[1-\frac{\varepsilon}{\kappa}\left(\boldsymbol{\Omega}\cdot\nabla\right)+\frac{\varepsilon^2}{\kappa^2}\left(\boldsymbol{\Omega}\cdot\nabla\right)^2-\frac{\varepsilon^3}{\kappa^3}\left(\boldsymbol{\Omega}\cdot\nabla\right)^3+\ldots\right]B(\nu,T)
\end{aligned} \tag{2.6}$$

Now we integrate both sides over a unit sphere.

$$\begin{aligned}
\int_{S^2}I\,d\boldsymbol{\Omega}&=\int_{S^2}\left[1-\frac{\varepsilon}{\kappa}\left(\boldsymbol{\Omega}\cdot\nabla\right)+\frac{\varepsilon^2}{\kappa^2}\left(\boldsymbol{\Omega}\cdot\nabla\right)^2-\frac{\varepsilon^3}{\kappa^3}\left(\boldsymbol{\Omega}\cdot\nabla\right)^3+\ldots\right]B\,d\boldsymbol{\Omega}\\
\varphi&=\int_{S^2}\left[1-\frac{\varepsilon}{\kappa}\left(\boldsymbol{\Omega}\cdot\nabla\right)+\frac{\varepsilon^2}{\kappa^2}\left(\boldsymbol{\Omega}\cdot\nabla\right)^2-\frac{\varepsilon^3}{\kappa^3}\left(\boldsymbol{\Omega}\cdot\nabla\right)^3+\ldots\right]d\boldsymbol{\Omega}B
\end{aligned} \tag{2.7}$$

On the left-hand side we obtain spherical intensity average, or in other words: energy flux. At this moment we have to dedicate some time to modify the right-hand side. First, we are able to move blackbody intensity out of the integral as it does not depend on direction $\boldsymbol{\Omega}$.

The next step involves employing an integral formula

$$\int_{S^2}(\boldsymbol{\Omega}\cdot\nabla)^n\,d\boldsymbol{\Omega}=\left[1+(-1)^n\right]\frac{2\pi}{n+1}\nabla^n. \tag{2.8}$$

In this chapter, we only show its application in deriving desired equations, the proof of the formula is provided in the attachment B.

2.1.1 Governing equations

In this section, we use result (2.8) to further simplify equation (2.7).

$$\varphi=4\pi\left[1+\frac{\varepsilon^2}{3\kappa^2}\nabla^2+\frac{\varepsilon^4}{5\kappa^4}\nabla^4+\frac{\varepsilon^6}{7\kappa^6}\nabla^6+\ldots\right]B \tag{2.9}$$

Here we use notation $\nabla^2=\nabla\cdot\nabla=\Delta$. The absence of odd terms allows for the desired diffusion approximation. However, we want the operators to act on the unknown function, φ in this case, not on B. We therefore invert everything

back to the left-hand side using the Neumann series once again.

$$
\begin{aligned}
4\pi B &= \left[1 + \frac{\varepsilon^2}{3\kappa^2}\nabla^2 + \frac{\varepsilon^4}{5\kappa^4}\nabla^4 + \frac{\varepsilon^6}{7\kappa^6}\nabla^6 + \dots\right]^{-1} \varphi \\
4\pi B &= \left[1 - \left(\frac{\varepsilon^2}{3\kappa^2}\nabla^2 + \frac{\varepsilon^4}{5\kappa^4}\nabla^4 + \frac{\varepsilon^6}{7\kappa^6}\nabla^6 + \dots\right) + \right. \\
&\quad + \left(\frac{\varepsilon^2}{3\kappa^2}\nabla^2 + \frac{\varepsilon^4}{5\kappa^4}\nabla^4 + \frac{\varepsilon^6}{7\kappa^6}\nabla^6 + \dots\right)^2 - \\
&\quad \left. - \left(\frac{\varepsilon^2}{3\kappa^2}\nabla^2 + \frac{\varepsilon^4}{5\kappa^4}\nabla^4 + \frac{\varepsilon^6}{7\kappa^6}\nabla^6 + \dots\right)^3 + \dots\right] \varphi
\end{aligned} \tag{2.10}
$$

Here we step in with the classic approximation technique, we neglect high order terms in our expansion. First, we clean up our formula a bit by gathering all the same order terms together and then we introduce "big O" notation.

$$
4\pi B = \left[1 - \frac{\varepsilon^2}{3\kappa^2}\nabla^2 - \frac{4\varepsilon^4}{45\kappa^4}\nabla^4 - \frac{44\varepsilon^6}{945\kappa^6}\nabla^6\right] \varphi + \mathcal{O}(\varepsilon^8) \tag{2.11}
$$

For illustration, we calculated the first three terms with error of order $\mathcal{O}(\varepsilon^8)$. Depending on the order of error, i.e. which terms we choose to neglect, we get different $\mathrm{SP_n}$ models. This paper is further dedicated mainly to $\mathrm{SP_1}$ equations which correspond to approximation up to $\mathcal{O}(\varepsilon^4)$.

$$
4\pi B = \left[1 - \frac{\varepsilon^2}{3\kappa^2}\nabla^2\right] \varphi + \mathcal{O}(\varepsilon^4) \tag{2.12}
$$

We can see that we have obtained an equation not for the original unknown function I, but its spherical average φ instead. An important fact is that this new quantity is no longer dependent on direction, so if we are able to adjust the coupling of governing equations, we successfully get rid of one of the problematic variables.

Here we hugely appreciate the genius behind this method. The coupling term that relates equations (2.3a) and (2.3b) reads

$$
\int_{\nu_1}^{\infty} \int_{S^2} \kappa\Big(B(\nu, T) - I(\mathbf{x}, t, \mathbf{\Omega}, \nu)\Big)\, d\mathbf{\Omega}\, d\nu. \tag{2.13}
$$

The only form in which the intensity is present here is exactly in its directional average over the unit sphere. We can simply replace it with the new unknown function φ and completely forget about direction-dependency.

$$
\int_{\nu_1}^{\infty} 4\pi\kappa B(\nu, T) - \kappa\varphi(\mathbf{x}, t, \nu)\, d\nu \tag{2.14}
$$

This term can be finally modified by substituting from (2.12)

$$
-\varepsilon^2 \int_{\nu_1}^{\infty} \frac{1}{3\kappa}\nabla^2\varphi(\mathbf{x}, t, \nu)\, d\nu + \mathcal{O}(\varepsilon^4) \tag{2.15}
$$

We can now install new coupling term (2.15) into (2.3a). We can see that in reality, this equation is only $\mathcal{O}(\varepsilon^2)$ after cancellation.

$$\begin{aligned}\varepsilon^2\frac{\partial T(\mathbf{x},t)}{\partial t} &= \varepsilon^2\nabla\cdot(k\nabla T(\mathbf{x},t)) + \varepsilon^2\int_{\nu_1}^{\infty}\frac{1}{3\kappa}\nabla^2\varphi(\mathbf{x},t,\nu)\,d\nu + \mathcal{O}(\varepsilon^4)\\ \frac{\partial T(\mathbf{x},t)}{\partial t} &= \nabla\cdot(k\nabla T(\mathbf{x},t)) + \int_{\nu_1}^{\infty}\frac{1}{3\kappa}\nabla^2\varphi(\mathbf{x},t,\nu)\,d\nu + \mathcal{O}(\varepsilon^2)\end{aligned} \tag{2.16}$$

If we combine this result with equation (2.12), we get complete bulk SP_1 equations

Bulk SP_1 equations

$$\frac{\partial T(\mathbf{x},t)}{\partial t} = \nabla\cdot(k\nabla T(\mathbf{x},t)) + \int_{\nu_1}^{\infty}\nabla\cdot\frac{1}{3\kappa}\nabla\varphi(\mathbf{x},t,\nu)\,d\nu \tag{2.17}$$

$$-\varepsilon^2\nabla\cdot\frac{1}{3\kappa}\nabla\varphi(\mathbf{x},t,\nu) + \kappa\varphi(\mathbf{x},t,\nu) = \kappa(4\pi B(\nu,T)) \tag{2.18}$$

Note that we have rewritten the Laplace operator in the original form of a divergence of gradient, putting the coefficient κ inside. This is the correct form for situations when κ is spatially dependent coefficient. In chapter 4, we conduct several numerical experiments also considering setting with non-constant κ, then this modification becomes necessary.

2.1.2 Rosseland approximation

Before we proceed with complementary boundary equations, we stop to investigate an interesting idea. Because the equation (2.18) is approximation of order $\mathcal{O}(\varepsilon^2)$, nothing goes wrong if we substitute from relation

$$4\pi B = \varphi + \mathcal{O}(\varepsilon^2) \tag{2.19}$$

with the same order of error. This equation is easily obtained from equation (2.11) by neglecting every but one term in expansion. By this maneuver, we eliminate the complex intensity field altogether and we are left with a simple blackbody approximation. It means that the problem is significantly simplified and reduced to only one unknown function $T(\mathbf{x},t)$ and one diffusion equation.

$$\frac{\partial T(\mathbf{x},t)}{\partial t} = \nabla\cdot(k\nabla T(\mathbf{x},t)) + \int_{\nu_1}^{\infty}\nabla\cdot\frac{4\pi}{3\kappa}\nabla B(\nu,T)\,d\nu \tag{2.20}$$

Using the chain rule results in a simple heat equation only with one extra term representing a contribution of thermal radiation. The full system, known as the Rosseland approximation (Frank and Klar [2011], p. 96), when written including the (thermal) boundary conditions reads as follows

Rosseland approximation

$$\frac{\partial T(\mathbf{x},t)}{\partial t} = \nabla\cdot\left(k + \frac{4\pi}{3\kappa}\int_{\nu_1}^{\infty}\frac{\partial B(\nu,T)}{\partial T}\,d\nu\right)\nabla T(\mathbf{x},t) \tag{2.21a}$$

$$\varepsilon k(\mathbf{n}\cdot\nabla)T(\mathbf{x},t) = h\left(T_b - T(\mathbf{x},t)\right) + \alpha\pi\int_0^{\nu_1} B_b(\nu,T_b) - B_b(\nu,T)\,d\nu \tag{2.21b}$$

2.1.3 Boundary conditions

We may have switched the unknown function from I to φ in bulk equations, but our boundary conditions still remain in the old form with direction as one of the variables. In this section, we derive desired boundary condition for quantity φ. This is one of the main contributions of this paper because the procedure is not trivial at all. We proceed with asymptotic derivation which is not commonly discussed in literature. As we stated at the beginning of chapter 2, one can approach the whole (RTE) system with tools of the calculus of variations and end up with $\mathrm{SP_n}$ equations. The same holds for the boundary conditions and that is usually the resource for most papers regarding this topic.

Here, we present, in a detailed manner, a procedure how to obtain the same equations via asymptotic expansion. It allows us to get a clearer insight into individual terms in the boundary conditions and additionally, our derivation makes it possible for us to constitute even transition conditions on the interface between two mediums with different refractive indices for multiple-domain problems.

Let us start with the derivation. Our goal is to transform an equation (1.41b):

$$I(\mathbf{x},t,\mathbf{\Omega},\nu) = \rho_1(|\mathbf{n}\cdot\mathbf{\Omega}'|)I(\mathbf{x},t,\mathbf{\Omega}'\nu) + [1-\rho_2(|\mathbf{n}\cdot\mathbf{\Omega}_i|)]\left(\frac{n_1}{n_2}\right)^2 B_b(\nu,T_b) \quad (2.22)$$

into one concerning φ.

The idea is to calculate the normal component of the radiative flux generated by intensity terms. We are driven by the vision of an integral average of intensity. But since we are situated on the boundary, it turns out that we do not have to integrate over the whole sphere, but hemisphere orientated into medium $\mathcal{M}_1$ ($\mathbf{n}\cdot\mathbf{\Omega} < 0$) does suffice. Let us denote this hemisphere H^2_-. Although we say we integrate over this hemisphere, our spherical variables $\phi \in (0, 2\pi)$ and $\theta \in (0, \frac{\pi}{2})$ in fact parametrize the other half. In other words, we consider $\mathbf{\Omega}$ to equal

$$\mathbf{\Omega} = \begin{pmatrix} \cos(\phi)\sin(\theta) \\ \sin(\phi)\sin(\theta) \\ -\cos(\theta) \end{pmatrix}, \qquad \text{specially } \mathbf{n} = \begin{pmatrix} 0 \\ 0 \\ 1 \end{pmatrix}. \quad (2.23)$$

We are interested in knowing the normal part of the heat flux, we multiply the equation (2.22) by $(\mathbf{n}\cdot\mathbf{\Omega})$ and then take an integral over H^2_-. Quick note, we omit excessive function arguments for the sake of simplicity of notation.

$$\begin{aligned}\int_{H^2_-} (\mathbf{n}\cdot\mathbf{\Omega})I(\mathbf{\Omega})\,d\mathbf{\Omega} = &\int_{H^2_-} (\mathbf{n}\cdot\mathbf{\Omega})\rho_1(|\mathbf{n}\cdot\mathbf{\Omega}'|)I(\mathbf{\Omega}')\,d\mathbf{\Omega} + \\ &+ \int_{H^2_-} (\mathbf{n}\cdot\mathbf{\Omega})\left[1-\rho_2(|\mathbf{n}\cdot\mathbf{\Omega}_i|)\right]\left(\frac{n_1}{n_2}\right)^2 B_b\,d\mathbf{\Omega} \end{aligned} \quad (2.24)$$

Let us now dissect this equation (2.24) term by term and rigorously calculate the result. Right at the first integral on the left-hand side we bump into a problem, we don't know the intensity I as a function of $\mathbf{\Omega}$, hence we can't calculate that integral. Here we apply the first trick, we employ the asymptotic expansion (2.6) again as promised and deduce this relation

$$I(\mathbf{\Omega}) = \left[1 - \frac{\varepsilon}{\kappa}(\mathbf{\Omega}\cdot\nabla)\right] B. \quad (2.25)$$

Note that there is an error of order $\mathcal{O}(\varepsilon^2)$ which is exactly the order we aim at with SP_1 equations, see (2.16).

We can substitute this in (2.24) and make it at the very least possible for us to try to calculate those integrals. The following pages contain in-depth derivation of the SP_1 boundary conditions, they are summarized in (2.54) on page 28.

Left-hand side

First, we calculate the integral on the left-hand side.

$$\int_{H^2_-} (\mathbf{n}\cdot\boldsymbol{\Omega}) I(\boldsymbol{\Omega})\, d\boldsymbol{\Omega} = \int_{H^2_-} (\mathbf{n}\cdot\boldsymbol{\Omega}) \left[1 - \frac{\varepsilon}{\kappa}(\boldsymbol{\Omega}\cdot\nabla)\right] B\, d\boldsymbol{\Omega} \tag{2.26}$$

The blackbody radiation function is together with the nabla operator no longer dependent on $\boldsymbol{\Omega}$, so after splitting into two integrals it can be factored outside of the integral.

$$\ldots = \int_{H^2_-} (\mathbf{n}\cdot\boldsymbol{\Omega})\, d\boldsymbol{\Omega} B - \frac{\varepsilon}{\kappa} \int_{H^2_-} (\mathbf{n}\cdot\boldsymbol{\Omega})\boldsymbol{\Omega}\, d\boldsymbol{\Omega}\cdot\nabla B \tag{2.27}$$

The first integral is already trivial, in the second one the integrand is a vector, therefore we integrate every component separately.

$$\begin{aligned} &= \int_0^{2\pi}\int_0^{\frac{\pi}{2}} -\cos(\theta)\sin(\theta)\, d\theta\, d\phi B \\ &\qquad - \frac{\varepsilon}{\kappa}\int_0^{2\pi}\int_0^{\frac{\pi}{2}} -\cos(\theta) \begin{pmatrix} \cos(\phi)\sin(\theta) \\ \sin(\phi)\sin(\theta) \\ -\cos(\theta) \end{pmatrix} \sin(\theta)\, d\theta\, d\phi \cdot \nabla B = \\ &= -2\pi\int_0^1 \mu\, d\mu B - 2\pi\frac{\varepsilon}{\kappa}\int_0^1 \mu^2\, d\mu \begin{pmatrix} 0 \\ 0 \\ 1 \end{pmatrix} \cdot \nabla B = -\pi B - \pi\frac{2\varepsilon}{3\kappa}(\mathbf{n}\cdot\nabla)B \end{aligned} \tag{2.28}$$

In the process, we adopted a simple substitution $\mu = \cos(\theta)$ that simplified our notation. Note that the first two components in the second integral have vanished because we have integrated $\cos(\phi)$ and $\sin(\phi)$ resp. from 0 to 2π.

Right-hand side

At the beginning of this subsection, we stop to define auxiliary integrals that appear in our results.

$$r_1^{(1)} = \int_0^1 \mu\rho_1(\mu)\, d\mu \qquad r_2^{(1)} = \int_0^1 \mu\rho_2(\mu)\, d\mu \tag{2.29}$$

$$r_1^{(2)} = \int_0^1 \mu^2\rho_1(\mu)\, d\mu \qquad r_2^{(2)} = \int_0^1 \mu^2\rho_2(\mu)\, d\mu \tag{2.30}$$

$$r_1^{(3)} = \int_0^1 \mu^3\rho_1(\mu)\, d\mu \qquad r_2^{(3)} = \int_0^1 \mu^3\rho_2(\mu)\, d\mu \tag{2.31}$$

Remind ourselves that ρ_1, resp. ρ_2, is reflectivity of the boundary for radiation incoming from $\mathcal{M}_1$, resp. $\mathcal{M}_2$. In our case, we of course work with $\mathcal{M}_2$ being a blackbody-like reservoir, ergo $\mathcal{M}_b$, so its moments will be later (in final formula (2.54)) renamed to $r_b^{(1)}$ and so on.

We continue with the first integral on the right-hand side of equation (2.24).

$$\int_{H^2_-} (\mathbf{n}\cdot\boldsymbol{\Omega})\rho_1(|\mathbf{n}\cdot\boldsymbol{\Omega}'|)I(\boldsymbol{\Omega}')\,d\boldsymbol{\Omega} \tag{2.32}$$

Recall relation (1.28) and see that

$$\boldsymbol{\Omega}' = \begin{pmatrix}\cos(\phi)\sin(\theta)\\ \sin(\phi)\sin(\theta)\\ \cos(\theta)\end{pmatrix}. \tag{2.33}$$

After substituting from (2.25) the integral reads

$$\begin{aligned}&\int_{H^2_-} (\mathbf{n}\cdot\boldsymbol{\Omega})\rho_1(|\mathbf{n}\cdot\boldsymbol{\Omega}'|)\left[1-\frac{\varepsilon}{\kappa}(\boldsymbol{\Omega}'\cdot\nabla)\right]B\,d\boldsymbol{\Omega} =\\ &= \int_{H^2_-} (\mathbf{n}\cdot\boldsymbol{\Omega})\rho_1(|\mathbf{n}\cdot\boldsymbol{\Omega}'|)\,d\boldsymbol{\Omega}B - \frac{\varepsilon}{\kappa}\int_{H^2_-} (\mathbf{n}\cdot\boldsymbol{\Omega})\rho_1(|\mathbf{n}\cdot\boldsymbol{\Omega}'|)\boldsymbol{\Omega}'\,d\boldsymbol{\Omega}\cdot\nabla B\end{aligned} \tag{2.34}$$

Let us resolve the first integral. It is useful to realize that

$$\mathbf{n}\cdot\boldsymbol{\Omega}' = \mathbf{n}\cdot(\boldsymbol{\Omega}-2(\mathbf{n}\cdot\boldsymbol{\Omega})\mathbf{n}) = \mathbf{n}\cdot\boldsymbol{\Omega}-2(\mathbf{n}\cdot\boldsymbol{\Omega})(\mathbf{n}\cdot\mathbf{n}) = -\mathbf{n}\cdot\boldsymbol{\Omega}, \tag{2.35}$$

meaning in absolute value, they are the same. We can therefore write

$$\begin{aligned}&\int_{H^2_-} (\mathbf{n}\cdot\boldsymbol{\Omega})\rho_1(|\mathbf{n}\cdot\boldsymbol{\Omega}'|)\,d\boldsymbol{\Omega}B = \int_{H^2_-} (\mathbf{n}\cdot\boldsymbol{\Omega})\rho_1(|\mathbf{n}\cdot\boldsymbol{\Omega}|)\,d\boldsymbol{\Omega}B =\\ &= \int_0^{2\pi}\int_0^{\frac{\pi}{2}} -\cos(\theta)\rho_1(\cos(\theta))\sin(\theta)\,d\theta\,d\phi B = -2\pi\int_0^1 \mu\rho_1(\mu)\,d\mu B =\\ &= -2\pi r_1^{(1)}B,\end{aligned} \tag{2.36}$$

where we got to use the notation introduced by relation (2.29).

We continue with the second integral.

$$\begin{aligned}&-\frac{\varepsilon}{\kappa}\int_{H^2_-} (\mathbf{n}\cdot\boldsymbol{\Omega})\rho_1(|\mathbf{n}\cdot\boldsymbol{\Omega}'|)\boldsymbol{\Omega}'\,d\boldsymbol{\Omega}\cdot\nabla B =\\ &= -\frac{\varepsilon}{\kappa}\int_0^{2\pi}\int_0^{\frac{\pi}{2}} -\cos(\theta)\rho_1(\cos(\theta))\begin{pmatrix}\cos(\phi)\sin(\theta)\\ \sin(\phi)\sin(\theta)\\ \cos(\theta)\end{pmatrix}\sin(\theta)\,d\theta\,d\phi\cdot\nabla B =\\ &= 2\pi\frac{\varepsilon}{\kappa}\int_0^{\frac{\pi}{2}} \cos^2(\theta)\rho_1(\cos(\theta))\sin(\theta)\,d\theta(\mathbf{n}\cdot\nabla)B =\\ &= 2\pi\frac{\varepsilon}{\kappa}\int_0^1 \mu^2\rho_1(\mu)\,d\mu(\mathbf{n}\cdot\nabla)B = 2\pi\frac{\varepsilon}{\kappa}r_1^{(2)}(\mathbf{n}\cdot\nabla)B\end{aligned} \tag{2.37}$$

For the vector integration, we have employed a procedure similar to (2.28). By putting (2.36) and (2.37) together, we obtain

$$\int_{H^2_-} (\mathbf{n}\cdot\boldsymbol{\Omega})\rho_1(|\mathbf{n}\cdot\boldsymbol{\Omega}'|)I(\boldsymbol{\Omega}')\,d\boldsymbol{\Omega} = -2\pi r_1^{(1)}B + 2\pi\frac{\varepsilon}{\kappa}r_1^{(2)}(\mathbf{n}\cdot\nabla)B \tag{2.38}$$

Now we turn our attention to the last integral from (2.24),

$$\int_{H^2_-} (\mathbf{n}\cdot\boldsymbol{\Omega})\left[1-\rho_2(|\mathbf{n}\cdot\boldsymbol{\Omega}_i|)\right]\left(\frac{n_1}{n_2}\right)^2 B_b\,d\boldsymbol{\Omega} \tag{2.39}$$

We notice the presence of direction $\mathbf{\Omega}_i$ in argument of reflectivity ρ_2. Unlike $\mathbf{\Omega}'$ it has no simple relation to $\mathbf{\Omega}$, thus integrating with respect to $\mathbf{\Omega}$ is not ideal (there is a way to do it discussed at the top of p. 27). We rewrite the integral in form

$$\left(\frac{n_1}{n_2}\right)^2 \int_0^{2\pi} \int_0^{\frac{\pi}{2}} -\cos(\theta)\,[1-\rho_2(\cos(\theta_i))]\sin(\theta)\,d\theta\,d\phi\,B_b \tag{2.40}$$

The main problem here is that due to the difference in refractive indices between $\mathcal{M}_1$ and $\mathcal{M}_b$ the hemisphere H^2_- parametrized by direction $\mathbf{\Omega}$ does not correspond well to hemisphere parametrized by $\mathbf{\Omega}_i$. We know that if we take full hemisphere in the optically thinner medium, then it transforms only into a spherical sector determined by a critical angle from Snell's law. This reminds us of our discussion about the shrinking cone of rays. In fact, we can use substitution (1.30) and after assigning $\theta_1 \to \theta, \theta_2 \to \theta_i$ transform our coordinates into hemisphere parametrized by $\mathbf{\Omega}_i$.

However, for the sake of rigor, we first employ the following identity

$$\rho_2(\cos(\theta_i)) = \rho_1(\cos(\theta)), \tag{2.41}$$

which follows directly from Snell's law (1.24) and Fresnel's equations (1.25) and (1.26) after incorporating relation

$$\cos(\theta) = \sqrt{1-\left(\frac{n_2}{n_1}\right)^2 (1-\cos(\theta_i))^2}. \tag{2.42}$$

Then the integral reads

$$\left(\frac{n_1}{n_2}\right)^2 \int_0^{2\pi} \int_0^{\frac{\pi}{2}} -\cos(\theta)\,[1-\rho_1(\cos(\theta))]\sin(\theta)\,d\theta\,d\phi\,B_b. \tag{2.43}$$

If we take a closer look at formula (1.25), we can deduce that the bracket here in integrand is zero for $\theta \in (\theta_c, \frac{\pi}{2})$, where θ_c is so called critical angle defined as $\sin(\theta_c) = \frac{n_2}{n_1} \iff \cos(\theta_c) = \sqrt{1-\left(\frac{n_2}{n_1}\right)^2}$. That means nothing changes if we set θ_c as upper integration limit instead of $\frac{\pi}{2}$.

$$\left(\frac{n_1}{n_2}\right)^2 \int_0^{2\pi} \int_0^{\theta_c} -\cos(\theta)\,[1-\rho_1(\cos(\theta))]\sin(\theta)\,d\theta\,d\phi\,B_b \tag{2.44}$$

Now we can use substitution (1.30) and with proper rescaling of integration interval we obtain

$$\begin{aligned}&\int_0^{2\pi} \int_0^{\frac{\pi}{2}} -\cos(\theta_i)\,[1-\rho_1(\cos(\theta))]\sin(\theta_i)\,d\theta_i\,d\phi\,B_b = \\ &= \int_0^{2\pi} \int_0^{\frac{\pi}{2}} -\cos(\theta_i)\,[1-\rho_2(\cos(\theta_i))]\sin(\theta_i)\,d\theta_i\,d\phi\,B_b\end{aligned} \tag{2.45}$$

This integral can be split into two and calculated in a similar fashion as the previous ones.

$$-\int_0^{2\pi} \int_0^{\frac{\pi}{2}} \cos(\theta_i)\sin(\theta_i)\,d\theta_i\,d\phi\,B_b = -2\pi\int_0^1 \mu\,d\mu\,B_b = -\pi B_b \tag{2.46}$$

$$\int_0^{2\pi} \int_0^{\frac{\pi}{2}} \cos(\theta_i)\rho_2(\cos(\theta_i))\sin(\theta_i)\,d\theta_i\,d\phi\,B_b = 2\pi\int_0^1 \mu\rho_2(\mu)\,d\mu\,B_b = 2\pi r_2^{(1)} B_b \tag{2.47}$$

A little side comment, as we have hinted in this case the coordinate transformation can be avoided. If we have just calculated the integral from (2.43) directly, we would obtain the result

$$-\left(\frac{n_1}{n_2}\right)^2\left(1-2r_1^{(1)}\right)\pi B_b, \tag{2.48}$$

where the factor $\left(\frac{n_1}{n_2}\right)^2$ has not disappeared, because there is no substitution involved. However, it can be shown that

$$\left(\frac{n_1}{n_2}\right)^2\left(1-2r_1^{(1)}\right)=\left(1-2r_2^{(1)}\right), \tag{2.49}$$

giving us the same result and confidence about the correctness. The proof is quite straightforward, once again it utilizes substitution (1.30) and the procedure described on the previous page:

$$\begin{aligned}\left(\frac{n_1}{n_2}\right)^2\left(1-2r_1^{(1)}\right)&=2\left(\frac{n_1}{n_2}\right)^2\left(\frac{1}{2}-r_1^{(1)}\right)=2\left(\frac{n_1}{n_2}\right)^2\int_0^1\mu-\mu\rho_1(\mu)\,d\mu=\\&=2\left(\frac{n_1}{n_2}\right)^2\int_0^{\frac{\pi}{2}}\cos(\theta)\left(1-\rho_1(\cos(\theta))\sin(\theta)\,d\theta=\right.\\&=2\left(\frac{n_1}{n_2}\right)^2\int_0^{\theta_c}\cos(\theta)\left(1-\rho_1(\cos(\theta))\sin(\theta)\,d\theta=\right.\\&=2\int_0^{\frac{\pi}{2}}\cos(\theta_i)\left(1-\rho_1(\cos(\theta))\sin(\theta_i)\,d\theta_i=\right.\\&=2\int_0^{\frac{\pi}{2}}\cos(\theta_i)\left(1-\rho_2(\cos(\theta_i))\sin(\theta_i)\,d\theta_i=\right.\\&=2\int_0^1\mu\left(1-\rho_2(\mu)\right)\,d\mu=2\left(\frac{1}{2}-r_2^{(1)}\right)=\left(1-2r_2^{(1)}\right)\end{aligned} \tag{2.50}$$

Why we have chosen to prefer the coordinate transformation technique in the derivation of boundary conditions will be clear when we get to the general setting where the incoming radiation is direction-dependent. Then it is necessary to make this step to proceed.

We have successfully integrated the boundary equation (2.22) and obtained several minor results that need to be reassembled. Particularly, we have calculated formulas (2.28) on the left-hand side and (2.38), (2.46) and (2.47) on the right-hand side.

$$-\pi B-\pi\frac{2\varepsilon}{3\kappa}(\mathbf{n}\cdot\nabla)B=-2\pi r_1^{(1)}B+2\pi\frac{\varepsilon}{\kappa}r_1^{(2)}(\mathbf{n}\cdot\nabla)B-\pi B_b+2\pi r_2^{(1)}B_b \tag{2.51}$$

We continue with some basic operations.

$$\left(1-2r_1^{(1)}\right)B+\frac{2\varepsilon}{3\kappa}\left(1+3r_1^{(2)}\right)(\mathbf{n}\cdot\nabla)B=\left(1-2r_2^{(1)}\right)B_b \tag{2.52}$$

Note that equation (2.52) does not involve quantity φ whatsoever for which we want the boundary condition to apply. We resort once again to the asymptotic expansion and use modified relation (2.19),

$$B=\frac{\varphi}{4\pi}+\mathcal{O}(\varepsilon^2). \tag{2.53}$$

The error order of $\mathcal{O}(\varepsilon^2)$ we hold for the entire SP_1 formulation and is therefore sufficient.

Thus we gain the final form of SP_1 intensity boundary condition.

SP_1 boundary condition

$$\left(1 - 2r_1^{(1)}\right)\varphi(\mathbf{x}, t, \nu) + \frac{2\varepsilon}{3\kappa}\left(1 + 3r_1^{(2)}\right)(\mathbf{n} \cdot \nabla)\varphi(\mathbf{x}, t, \nu) = \left(1 - 2r_b^{(1)}\right) 4\pi B_b(\nu, T_b) \tag{2.54}$$

Formulation (2.54) is similar to the ones presented in the literature, for example (Larsen et al. [2002], eq. (3.2)), only nuance is in term $\left(1 - 2r_b^{(1)}\right)$ on the right-hand side. It correctly accounts for the difference in refractive indices, reflectivities and their moments. In mentioned article, there is just $\left(1 - 2r_1^{(1)}\right)$ instead of it.

Temperature boundary condition (2.21b) does not require any modification.

2.1.4 Transition conditions

Up to now, we have only considered a simple problem of one domain with evolving temperature while the optically different surroundings is being fixed at constant temperature. Plus the incoming radiation is Planckian in distribution, ergo not direction-dependent. Such problem is fairly accurately described by many authors (Larsen et al. [2002]; Larsen et al. [2003]; Frank and Klar [2011]) in literature. Still we have managed to make several improvements concerning the boundary conditions, see (2.54).

However, now we turn to a little different setup. We still consider two mediums $\mathcal{M}_1$ and $\mathcal{M}_2$ with different refractive indexes in contact, but we allow the temperature to evolve freely in **both of them**. The heat transport is again modeled by conduction together with radiation, the only difference is that blackbody-like radiation from $\mathcal{M}_2$ is no longer good enough approximation and in both mediums, we consider direction-dependent intensity function, I_1 and I_2 resp.

In the bulk regions $\mathcal{M}_1$ and $\mathcal{M}_2$ not much changes. Equations (1.40a) and (1.40b) still hold and can be approximated with equations (2.17) and (2.18). Of course, now that we think of medium $\mathcal{M}_2$ as full-fledged domain of interest, we introduce a new set of parameters for $\mathcal{M}_1$ and $\mathcal{M}_2$, respectively; naturally κ_1 and κ_2 absorption coefficients, k_1 and k_2 thermal conductivity coefficients. In $\mathcal{M}_1$ we solve bulk equations with one set of parameters and in $\mathcal{M}_2$ with the other. In essence, we could say that the parameters κ and k became spatially dependent, although this dependence is very simple - piecewise constant functions.

The individual domains of $\mathcal{M}_1$ and $\mathcal{M}_2$ are bounded and on parts of their boundary which they do not share we can prescribe boundary conditions discussed in the previous section. In other words, we regard them as being surrounded by a reservoir $\mathcal{M}_b$ at a constant temperature. We can also picture the first setting with just one domain of interest divided into two optically different parts and a proper description of temperature and intensity behavior near the interface between them is required.

We shall start with the derivation of the transition conditions. We are looking

for equations to correctly couple functions I_1 and I_2 across the interface between $\mathcal{M}_1$ and $\mathcal{M}_2$. Let equation (1.35) be our starting point after distinguishing intensity for both sides of the interface.

$$I_1(\mathbf{x},t,\mathbf{\Omega},\nu) = \rho_1(|\mathbf{n}\cdot\mathbf{\Omega}'|)I_1(\mathbf{x},t,\mathbf{\Omega}',\nu) + [1-\rho_2(|\mathbf{n}\cdot\mathbf{\Omega}_i|)]\left(\frac{n_1}{n_2}\right)^2 I_2(\mathbf{x},t,\mathbf{\Omega}_i,\nu) \tag{2.55}$$

Not much has changed here compared with (2.22) because we have already accounted for the refraction in the first setting. Only, I_2 does have direction as an argument and B_b does not. This makes our calculation a tiny bit more complicated but not too much.

In our SP_1 bulk equations we work with average φ, hence we define

$$\varphi_1(\mathbf{x},t,\nu) = \int_{S^2} I_1(\mathbf{x},t,\mathbf{\Omega},\nu)\,d\mathbf{\Omega} \tag{2.56}$$

$$\varphi_2(\mathbf{x},t,\nu) = \int_{S^2} I_2(\mathbf{x},t,\mathbf{\Omega},\nu)\,d\mathbf{\Omega} \tag{2.57}$$

and we would like to gain a relationship between these two functions at the interface. They are two functions each solving second-order differential equations on separate domains. To couple them, two equations are required.

Since we have treated simpler boundary conditions with care, the ideas and techniques can now be applied also to the current setting. Therefore we proceed by calculating the radiative flux running through the boundary. We multiply the equation by $(\mathbf{n}\cdot\mathbf{\Omega})$ and integrate over the unit hemisphere H^2_-. All the notation is the same as introduced in section 2.1.3 (also we omit evident function arguments).

$$\begin{aligned}\int_{H^2_-}(\mathbf{n}\cdot\mathbf{\Omega})I_1(\mathbf{\Omega})\,d\mathbf{\Omega} = \int_{H^2_-}(\mathbf{n}\cdot\mathbf{\Omega})\rho_1(|\mathbf{n}\cdot\mathbf{\Omega}'|)I_1(\mathbf{\Omega}')\,d\mathbf{\Omega} + \\ + \left(\frac{n_1}{n_2}\right)^2\int_{H^2_-}(\mathbf{n}\cdot\mathbf{\Omega})\left[1-\rho_2(|\mathbf{n}\cdot\mathbf{\Omega}_i|)\right]I_2(\mathbf{\Omega}_i)\,d\mathbf{\Omega}\end{aligned} \tag{2.58}$$

We can see that integrals involving I_1 are identical to ones in equation (2.24) and we can straight write results analogous to (2.28) and (2.38).

$$\int_{H^2_-}(\mathbf{n}\cdot\mathbf{\Omega})I_1(\mathbf{\Omega})\,d\mathbf{\Omega} = -\pi B_1 - \pi\frac{2\varepsilon}{3\kappa_1}(\mathbf{n}\cdot\nabla)B_1 \tag{2.59}$$

$$\int_{H^2_-}(\mathbf{n}\cdot\mathbf{\Omega})\rho_1(|\mathbf{n}\cdot\mathbf{\Omega}'|)I_1(\mathbf{\Omega}')\,d\mathbf{\Omega} = -2\pi r_1^{(1)}B_1 + 2\pi\frac{\varepsilon}{\kappa_1}r_1^{(2)}(\mathbf{n}\cdot\nabla)B_1 \tag{2.60}$$

Note that we distinguish also between B_1 in $\mathcal{M}_1$ and B_2 in $\mathcal{M}_2$ as they do have refractive index n_1, resp. n_2, in their definition, recall (1.7).

The only thing left to do is to calculate the integral that has altered a bit. Now there is a direction-dependent function $I_2(\mathbf{\Omega}_i)$ instead of B_b.

$$\left(\frac{n_1}{n_2}\right)^2\int_{H^2_-}(\mathbf{n}\cdot\mathbf{\Omega})\left[1-\rho_2(|\mathbf{n}\cdot\mathbf{\Omega}_i|)\right]I_2(\mathbf{\Omega}_i)\,d\mathbf{\Omega} \tag{2.61}$$

According to the technique described within equations (2.40) up to (2.45) we transform the integration variable to $\mathbf{\Omega}_i$ and thus simplify the expressions.

$$\left(\frac{n_1}{n_2}\right)^2 \int_0^{2\pi}\int_0^{\frac{\pi}{2}} (\mathbf{n}\cdot\mathbf{\Omega})\left[1-\rho_2(|\mathbf{n}\cdot\mathbf{\Omega}_i|)\right] I_2(\mathbf{\Omega}_i)\sin(\theta)\,d\theta\,d\phi$$
$$\left(\frac{n_1}{n_2}\right)^2 \int_0^{2\pi}\int_0^{\frac{\pi}{2}} (\mathbf{n}\cdot\mathbf{\Omega})\left[1-\rho_1(|\mathbf{n}\cdot\mathbf{\Omega}|)\right] I_2(\mathbf{\Omega}_i)\sin(\theta)\,d\theta\,d\phi$$
$$\left(\frac{n_1}{n_2}\right)^2 \int_0^{2\pi}\int_0^{\theta_c} (\mathbf{n}\cdot\mathbf{\Omega})\left[1-\rho_1(|\mathbf{n}\cdot\mathbf{\Omega}|)\right] I_2(\mathbf{\Omega}_i)\sin(\theta)\,d\theta\,d\phi$$
$$\int_0^{2\pi}\int_0^{\frac{\pi}{2}} (\mathbf{n}\cdot\mathbf{\Omega}_i)\left[1-\rho_2(|\mathbf{n}\cdot\mathbf{\Omega}_i|)\right] I_2(\mathbf{\Omega}_i)\sin(\theta_i)\,d\theta_i\,d\phi$$
$$\int_{H^2_-} (\mathbf{n}\cdot\mathbf{\Omega}_i)\left[1-\rho_2(|\mathbf{n}\cdot\mathbf{\Omega}_i|)\right] I_2(\mathbf{\Omega}_i)\,d\mathbf{\Omega}_i \tag{2.62}$$

We proceed with substituting from asymptotic expansion

$$I_2(\mathbf{\Omega}_i) = \left[1-\frac{\varepsilon}{\kappa_2}(\mathbf{\Omega}_i\cdot\nabla)\right] B_2 \tag{2.63}$$

and obtain integral

$$\int_{H^2_-} (\mathbf{n}\cdot\mathbf{\Omega}_i)\left[1-\rho_2(|\mathbf{n}\cdot\mathbf{\Omega}_i|)\right]\left[1-\frac{\varepsilon}{\kappa_2}(\mathbf{\Omega}_i\cdot\nabla)\right] B_2\,d\mathbf{\Omega}_i \tag{2.64}$$

which can be split into four simple integrals and resolved individually.

$$\int_{H^2_-} (\mathbf{n}\cdot\mathbf{\Omega}_i)\,d\mathbf{\Omega}_i B_2 - \int_{H^2_-} (\mathbf{n}\cdot\mathbf{\Omega}_i)\rho_2(|\mathbf{n}\cdot\mathbf{\Omega}_i|)\,d\mathbf{\Omega}_i B_2 -$$
$$-\frac{\varepsilon}{\kappa_2}\int_{H^2_-} (\mathbf{n}\cdot\mathbf{\Omega}_i)\,\mathbf{\Omega}_i\,d\mathbf{\Omega}_i\cdot\nabla B_2 + \frac{\varepsilon}{\kappa_2}\int_{H^2_-} (\mathbf{n}\cdot\mathbf{\Omega}_i)\rho_2(|\mathbf{n}\cdot\mathbf{\Omega}_i|)\,\mathbf{\Omega}_i\,d\mathbf{\Omega}_i\cdot\nabla B_2 \tag{2.65}$$

All techniques used have already been explained in the previous section 2.1.3.

1.

$$\int_{H^2_-} (\mathbf{n}\cdot\mathbf{\Omega}_i)\,d\mathbf{\Omega}_i B_2 = \int_0^{2\pi}\int_0^{\frac{\pi}{2}} -\cos(\theta_i)\sin(\theta_i)\,d\theta_i\,d\phi B_2 =$$
$$= -2\pi\int_0^1 \mu\,d\mu B_2 = -\pi B_2 \tag{2.66}$$

2.

$$-\int_{H^2_-} (\mathbf{n}\cdot\mathbf{\Omega}_i)\rho_2(|\mathbf{n}\cdot\mathbf{\Omega}_i|)\,d\mathbf{\Omega}_i B_2 =$$
$$= -\int_0^{2\pi}\int_0^{\frac{\pi}{2}} -\cos(\theta_i)\rho_2(\cos(\theta_i))\sin(\theta_i)\,d\theta_i\,d\phi B_2 =$$
$$= 2\pi\int_0^1 \mu\rho_2(\mu)\,d\mu B_2 = 2\pi r_2^{(1)} B_2 \tag{2.67}$$

3.

$$-\frac{\varepsilon}{\kappa_2}\int_{H^2_-} (\mathbf{n}\cdot\mathbf{\Omega}_i)\,\mathbf{\Omega}_i\,d\mathbf{\Omega}_i\cdot\nabla B_2 =$$
$$= -\frac{\varepsilon}{\kappa_2}\int_0^{2\pi}\int_0^{\frac{\pi}{2}} -\cos(\theta_i)\begin{pmatrix}\cos(\phi)\sin(\theta_i)\\ \sin(\phi)\sin(\theta_i)\\ -\cos(\theta_i)\end{pmatrix}\sin(\theta_i)\,d\theta_i\,d\phi\cdot\nabla B_2 =$$
$$= -2\pi\frac{\varepsilon}{\kappa_2}\int \mu^2\,d\mu\,(\mathbf{n}\cdot\nabla)B_2 = -\pi\frac{2\varepsilon}{3\kappa_2}(\mathbf{n}\cdot\nabla)B_2 \tag{2.68}$$

4.

$$\frac{\varepsilon}{\kappa_2}\int_{H^2_-}(\mathbf{n}\cdot\boldsymbol{\Omega}_i)\rho_2(|\mathbf{n}\cdot\boldsymbol{\Omega}_i|)\,\boldsymbol{\Omega}_i\,d\boldsymbol{\Omega}_i\cdot\nabla B_2 =$$

$$=\frac{\varepsilon}{\kappa_2}\int_0^{2\pi}\int_0^{\frac{\pi}{2}}-\cos(\theta_i)\rho_2(|\mathbf{n}\cdot\boldsymbol{\Omega}_i|)\begin{pmatrix}\cos(\phi)\sin(\theta_i)\\ \sin(\phi)\sin(\theta_i)\\ -\cos(\theta_i)\end{pmatrix}\sin(\theta_i)\,d\theta_i\,d\phi\cdot\nabla B_2 =$$

$$=2\pi\frac{\varepsilon}{\kappa_2}\int_0^1\mu^2\rho_2(\mu)\,d\mu(\mathbf{n}\cdot\nabla)B_2=2\pi\frac{\varepsilon}{\kappa_2}r_2^{(2)}(\mathbf{n}\cdot\nabla)B_2 \tag{2.69}$$

Now let us assemble the whole equation together. On the left-hand side, we use our prepared result (2.59) and on the right we add to earlier calculated (2.60) new findings, from (2.66) up to (2.69).

$$-\pi B_1-\pi\frac{2\varepsilon}{3\kappa_1}(\mathbf{n}\cdot\nabla)B_1=-2\pi r_1^{(1)}B_1+2\pi\frac{\varepsilon}{\kappa_1}r_1^{(2)}(\mathbf{n}\cdot\nabla)B_1-$$
$$-\pi B_2+2\pi r_2^{(1)}B_2-\pi\frac{2\varepsilon}{3\kappa_2}(\mathbf{n}\cdot\nabla)B_2+2\pi\frac{\varepsilon}{\kappa_2}r_2^{(2)}(\mathbf{n}\cdot\nabla)B_2, \tag{2.70}$$

which can be rewritten in the form

$$\left(1-2r_1^{(1)}\right)B_1+\frac{2\varepsilon}{3\kappa_1}\left(1+3r_1^{(2)}\right)(\mathbf{n}\cdot\nabla)B_1=\left(1-2r_2^{(1)}\right)B_2$$
$$+\frac{2\varepsilon}{3\kappa_2}\left(1-3r_2^{(2)}\right)(\mathbf{n}\cdot\nabla)B_2 \tag{2.71}$$

Now we make a final touch and substitute φ for B according to relation (2.53).

$$\left(1-2r_1^{(1)}\right)\varphi_1+\frac{2\varepsilon}{3\kappa_1}\left(1+3r_1^{(2)}\right)(\mathbf{n}\cdot\nabla)\varphi_1=\left(1-2r_2^{(1)}\right)\varphi_2$$
$$+\frac{2\varepsilon}{3\kappa_2}\left(1-3r_2^{(2)}\right)(\mathbf{n}\cdot\nabla)\varphi_2 \tag{2.72}$$

Here we stop and think about our current result. We have stated that there is a need for two controlling equations to properly couple our elliptic equations (2.18), so far we have got one of them, (2.72). Quite naturally we ask ourselves how we can obtain the missing counterpart.

Note that the equation (2.72) is not entirely symmetric, the sign in front of one of the terms with normal derivative is flipped compared to the other side. This is a glimpse of hope that if we look at the boundary from the other side's perspective, we get another equation that is not degenerated and brings us useful information.

Let us do it rigorously, the flipped perspective yield equation

$$I_2(\mathbf{x},t,\overline{\boldsymbol{\Omega}},\nu)=\rho_2(\left|\overline{\mathbf{n}}\cdot\overline{\boldsymbol{\Omega}}'\right|)I_2(\mathbf{x},t,\overline{\boldsymbol{\Omega}}',\nu)+\left[1-\rho_1(\left|\overline{\mathbf{n}}\cdot\overline{\boldsymbol{\Omega}}_i\right|)\right]\left(\frac{n_2}{n_1}\right)^2 I_1(\mathbf{x},t,\overline{\boldsymbol{\Omega}}_i,\nu), \tag{2.73}$$

which is altered (2.55). Pay attention to our notation at the moment, $\overline{\boldsymbol{\Omega}}$ represents the direction of the ray going from boundary to medium $\mathcal{M}_2$, $\overline{\boldsymbol{\Omega}}'$ is the direction that gets reflected into $\overline{\boldsymbol{\Omega}}$, it sort of stands for established direction $\boldsymbol{\Omega}_i$. On the

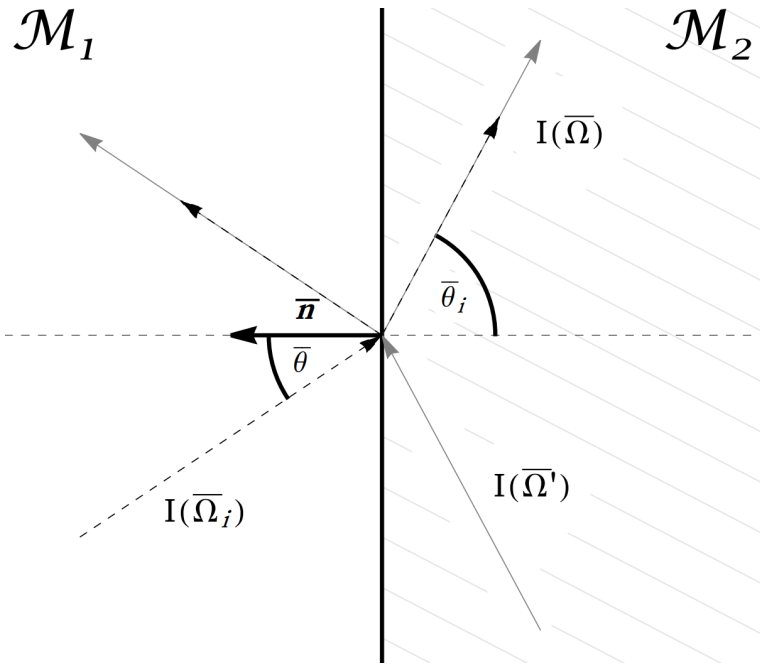

Figure 2.1: Boundary from other side's perspective

other hand, $\overline{\mathbf{\Omega}}_i$ is the direction coming from $\mathcal{M}_1$ that gets partially transmitted through. And $\overline{\mathbf{n}}$ is flipped normal vector, $\overline{\mathbf{n}} = -\mathbf{n}$. Every is depicted in figure 2.1.

The equation is multiplied by $(\overline{\mathbf{n}} \cdot \overline{\mathbf{\Omega}})$ and integrated over a hemisphere $\overline{H^2_-}$ where $\overline{\mathbf{\Omega}} \cdot \overline{\mathbf{n}} < 0$.

$$\int_{\overline{H^2_-}} (\overline{\mathbf{n}} \cdot \overline{\mathbf{\Omega}}) I_2(\overline{\mathbf{\Omega}})\, d\overline{\mathbf{\Omega}} = \int_{\overline{H^2_-}} (\overline{\mathbf{n}} \cdot \overline{\mathbf{\Omega}}) \rho_2(\left|\overline{\mathbf{n}} \cdot \overline{\mathbf{\Omega}}'\right|) I_2(\overline{\mathbf{\Omega}}')\, d\overline{\mathbf{\Omega}} + \\ + \int_{\overline{H^2_-}} (\overline{\mathbf{n}} \cdot \overline{\mathbf{\Omega}}) \left[1 - \rho_1(\left|\overline{\mathbf{n}} \cdot \overline{\mathbf{\Omega}}_i\right|)\right] \left(\frac{n_2}{n_1}\right)^2 I_1(\overline{\mathbf{\Omega}}_i)\, d\overline{\mathbf{\Omega}} \quad (2.74)$$

With the left-hand side integral and the first integral on the right-hand side, there is nothing extraordinary, we have already calculated such integrals before. With complete analogy, we refer to integrals (2.59) and (2.60).

$$\int_{\overline{H^2_-}} (\overline{\mathbf{n}} \cdot \overline{\mathbf{\Omega}}) I_2(\overline{\mathbf{\Omega}})\, d\overline{\mathbf{\Omega}} = -\pi B_2 - \pi \frac{2\varepsilon}{3\kappa_2} (\overline{\mathbf{n}} \cdot \nabla) B_2 \quad (2.75)$$

$$\int_{\overline{H^2_-}} (\overline{\mathbf{n}} \cdot \overline{\mathbf{\Omega}}) \rho_2(\left|\overline{\mathbf{n}} \cdot \overline{\mathbf{\Omega}}'\right|) I_2(\overline{\mathbf{\Omega}}')\, d\overline{\mathbf{\Omega}} = -2\pi r_2^{(1)} B_2 + 2\pi \frac{\varepsilon}{\kappa_2} r_2^{(2)} (\overline{\mathbf{n}} \cdot \nabla) B_2 \quad (2.76)$$

The last integral does call for coordinate transform so we integrate with respect to $\overline{\mathbf{\Omega}}_i$. For that we recall substitution (1.30), the angles playing roles are

now $\theta_2 = \overline{\theta}$ where $\cos\left(\overline{\theta}\right) = -\overline{\mathbf{n}} \cdot \overline{\mathbf{\Omega}}$ and $\theta_1 = \overline{\theta}_i$ where $\cos\left(\overline{\theta}_i\right) = -\overline{\mathbf{n}} \cdot \overline{\mathbf{\Omega}}_i$.

$$\int_{\overline{H^2_-}} (\overline{\mathbf{n}} \cdot \overline{\mathbf{\Omega}}) \left[1 - \rho_1(\left|\overline{\mathbf{n}} \cdot \overline{\mathbf{\Omega}}_i\right|)\right] \left(\frac{n_2}{n_1}\right)^2 I_1(\overline{\mathbf{\Omega}}_i)\, d\overline{\mathbf{\Omega}}$$

$$\left(\frac{n_2}{n_1}\right)^2 \int_0^{2\pi} \int_0^{\frac{\pi}{2}} -\cos\left(\overline{\theta}\right) \left[1 - \rho_1(\left|\overline{\mathbf{n}} \cdot \overline{\mathbf{\Omega}}_i\right|)\right] I_1(\overline{\mathbf{\Omega}}_i) \sin\left(\overline{\theta}\right) d\overline{\theta}\, d\overline{\phi}$$

$$\int_0^{2\pi} \int_0^{\overline{\theta}_{ic}} -\cos\left(\overline{\theta}_i\right) \left[1 - \rho_1(\left|\overline{\mathbf{n}} \cdot \overline{\mathbf{\Omega}}_i\right|)\right] I_1(\overline{\mathbf{\Omega}}_i) \sin\left(\overline{\theta}_i\right) d\overline{\theta}_i\, d\overline{\phi}$$

$$\int_0^{2\pi} \int_0^{\frac{\pi}{2}} -\cos\left(\overline{\theta}_i\right) \left[1 - \rho_1(\left|\overline{\mathbf{n}} \cdot \overline{\mathbf{\Omega}}_i\right|)\right] I_1(\overline{\mathbf{\Omega}}_i) \sin\left(\overline{\theta}_i\right) d\overline{\theta}_i\, d\overline{\phi}$$

$$\int_{\overline{H^2_-}} (\overline{\mathbf{n}} \cdot \overline{\mathbf{\Omega}}_i) \left[1 - \rho_1(\left|\overline{\mathbf{n}} \cdot \overline{\mathbf{\Omega}}_i\right|)\right] I_1(\overline{\mathbf{\Omega}}_i)\, d\overline{\mathbf{\Omega}_i} \tag{2.77}$$

This final integral is also familiar. It is analogous to one from (2.61) and calculations can be carried out as follows in (2.62) up to (2.69).

$$\ldots = -\pi B_1 + 2\pi r_1^{(1)} B_1 - \pi \frac{2\varepsilon}{3\kappa_1} (\overline{\mathbf{n}} \cdot \nabla) B_1 + 2\pi \frac{\varepsilon}{\kappa_1} r_1^{(2)} (\overline{\mathbf{n}} \cdot \nabla) B_1 \tag{2.78}$$

We can see that by switching the perspective to the other side, the calculations themselves do not in principle change a bit. In fact, we could just take equation (2.70) and interchange indices 1 and 2 regarding mediums $\mathcal{M}_1$ and $\mathcal{M}_2$ and we would obtain same result.

$$\begin{aligned} -\pi B_2 - \pi \frac{2\varepsilon}{3\kappa_2} (\overline{\mathbf{n}} \cdot \nabla) B_2 = -2\pi r_2^{(1)} B_2 + 2\pi \frac{\varepsilon}{\kappa_2} r_2^{(2)} (\overline{\mathbf{n}} \cdot \nabla) B_2 - \\ - \pi B_1 + 2\pi r_1^{(1)} B_1 - \pi \frac{2\varepsilon}{3\kappa_1} (\overline{\mathbf{n}} \cdot \nabla) B_1 + 2\pi \frac{\varepsilon}{\kappa_1} r_1^{(2)} (\overline{\mathbf{n}} \cdot \nabla) B_1 \end{aligned} \tag{2.79}$$

However, we are dealing with somewhat new theory and formulas not written in available literature, thus rigor is our priority.

After reassembling the terms, we get the equation into a more condensed form.

$$\begin{aligned} \left(1 - 2r_2^{(1)}\right) B_2 + \frac{2\varepsilon}{3\kappa_2} \left(1 + 3r_2^{(2)}\right) (\overline{\mathbf{n}} \cdot \nabla) B_2 = \left(1 - 2r_1^{(1)}\right) B_1 \\ + \frac{2\varepsilon}{3\kappa_1} \left(1 - 3r_1^{(2)}\right) (\overline{\mathbf{n}} \cdot \nabla) B_1 \end{aligned} \tag{2.80}$$

We would like to compare this equation with (2.72) (here we write again for better clarity as (2.82)), the one transition condition already obtained. We therefore switch sides of the equation, substituting φ_1 and φ_2 according to (2.53). Lastly we see the derivative $\overline{\mathbf{n}} \cdot \nabla$ still differs from $\mathbf{n} \cdot \nabla$, to solve this we just use relation $\overline{\mathbf{n}} = -\mathbf{n}$ and obtain the second transition condition

$$\begin{aligned} \left(1 - 2r_1^{(1)}\right) \varphi_1 - \frac{2\varepsilon}{3\kappa_1} \left(1 - 3r_1^{(2)}\right) (\mathbf{n} \cdot \nabla) \varphi_1 = \left(1 - 2r_2^{(1)}\right) \varphi_2 \\ - \frac{2\varepsilon}{3\kappa_2} \left(1 + 3r_2^{(2)}\right) (\mathbf{n} \cdot \nabla) \varphi_2. \end{aligned} \tag{2.81}$$

Here we state the first condition (2.72) as a reminder:

$$\begin{aligned} \left(1 - 2r_1^{(1)}\right) \varphi_1 + \frac{2\varepsilon}{3\kappa_1} \left(1 + 3r_1^{(2)}\right) (\mathbf{n} \cdot \nabla) \varphi_1 = \left(1 - 2r_2^{(1)}\right) \varphi_2 \\ + \frac{2\varepsilon}{3\kappa_2} \left(1 - 3r_2^{(2)}\right) (\mathbf{n} \cdot \nabla) \varphi_2 \end{aligned} \tag{2.82}$$

We have achieved our desired goal that is obtained two independent transition conditions for functions φ_1 and φ_2. We can subtract or add those equations to get form that is a little more clear and does not seem fully arbitrary.

SP_1 transition conditions

$$\frac{1}{\kappa_1}(\mathbf{n}\cdot\nabla)\varphi_1 = \frac{1}{\kappa_2}(\mathbf{n}\cdot\nabla)\varphi_2 \tag{2.83}$$

$$\left(1-2r_1^{(1)}\right)\varphi_1 + \frac{2\varepsilon}{\kappa_1}r_1^{(2)}(\mathbf{n}\cdot\nabla)\varphi_1 = \left(1-2r_2^{(1)}\right)\varphi_2 - \frac{2\varepsilon}{\kappa_2}r_2^{(2)}(\mathbf{n}\cdot\nabla)\varphi_2 \tag{2.84}$$

where $\varphi_1 = \varphi_1(\mathbf{x}, t, \nu)$ (same for φ_2) and these equations hold for all $\mathbf{x}$ on the boundary between mediums $\mathcal{M}_1$ and $\mathcal{M}_2$.

After all manipulations, a subtle asymmetry still persists in formula (2.84). It looks like there has to be an error deep in our thinking when we got an asymmetric result. Common sense tells us that if $\mathcal{M}_1$ and $\mathcal{M}_2$ are identical regarding κ and n, then functions φ_1 and φ_2 should be identical, in other words, the whole situation should be symmetric along the boundary. Here we can be relieved because in our model, once there is no difference in refractive indices n_1 and n_2, the reflectivities ρ_1 and ρ_2 are both zero functions and the system behaves as if there is no boundary whatsoever. At that moment the transition conditions (2.83) and (2.84) become simpler and read

$$(\mathbf{n}\cdot\nabla)\varphi_1 = (\mathbf{n}\cdot\nabla)\varphi_2 \tag{2.85}$$

$$\varphi_1 = \varphi_2 \tag{2.86}$$

This means that derived equations are also consistent with the basic assumptions we lay on the model. The asymmetry in transition conditions stems solely from the specified direction of $\mathbf{n}$.

2.1.5 SP_1 summary

Let us now summarize the idea and formulas of SP_1 approximations. The full (RTE) system properly describing radiative heat transport is very difficult to solve directly, therefore we need simpler theoretical approximations. One of the many possibilities are just the SP_n equations. Using them, we consider the complex transport of radiation being replaced by a diffusive one and thus allowing the direction-dependency to disappear.

We have asymptotically derived the bulk SP_1 equations by following steps discovered by other authors in the literature (Larsen et al. [2002]).

Then we supplemented them with appropriate boundary conditions which we derived asymptotically on our own. These are applied to boundaries between two mediums where one represents the problem domain itself and the other is just a thermal black-body reservoir.

On top of that, we have also generalized the boundary conditions for interfaces between two mediums within the domain of interest with each having its own refracting index and coefficient of absorption. These are the transition conditions.

Note that the temperature function is not directly affected by multiple refractive mediums. The only impact is through a complex intensity field that plays its

role in the evolutionary equation. Therefore we do not need any special temperature transition conditions and we use the traditional assumptions of continuity of temperature and of the normal heat flux.

$\mathbf{SP_1}$ approximation

Bulk equations

$$\frac{\partial T(\mathbf{x},t)}{\partial t} = \nabla \cdot (k \nabla T(\mathbf{x},t)) + \int_{\nu_1}^{\infty} \nabla \cdot \frac{1}{3\kappa} \nabla \varphi(\mathbf{x},t,\nu)\, d\nu \tag{2.87a}$$

$$-\varepsilon^2 \nabla \cdot \frac{1}{3\kappa} \nabla \varphi(\mathbf{x},t,\nu) + \kappa \varphi(\mathbf{x},t,\nu) = \kappa (4\pi B(\nu,T)) \tag{2.87b}$$

Temperature boundary condition

$$\varepsilon k (\mathbf{n} \cdot \nabla) T(\mathbf{x},t) = h\,(T_b - T(\mathbf{x},t)) + \alpha\pi \int_0^{\nu_1} B_b(\nu,T_b) - B_b(\nu,T)\, d\nu \tag{2.87c}$$

Temperature transition conditions

$$T_1(\mathbf{x},t) = T_2(\mathbf{x},t) \tag{2.87d}$$

$$k_1 (\mathbf{n} \cdot \nabla) T_1(\mathbf{x},t) = k_2 (\mathbf{n} \cdot \nabla) T_2(\mathbf{x},t) \tag{2.87e}$$

Intensity boundary condition

$$\left(1 - 2r_1^{(1)}\right) \varphi + \frac{2\varepsilon}{3\kappa} \left(1 + 3r_1^{(2)}\right) (\mathbf{n} \cdot \nabla) \varphi = \left(1 - 2r_b^{(1)}\right) 4\pi B_b(\nu,T_b) \tag{2.87f}$$

Intensity transition conditions

$$\frac{1}{\kappa_1} (\mathbf{n} \cdot \nabla) \varphi_1 = \frac{1}{\kappa_2} (\mathbf{n} \cdot \nabla) \varphi_2 \tag{2.87g}$$

$$\left(1 - 2r_1^{(1)}\right) \varphi_1 + \frac{2\varepsilon}{\kappa_1} r_1^{(2)} (\mathbf{n} \cdot \nabla) \varphi_1 = \left(1 - 2r_2^{(1)}\right) \varphi_2 - \frac{2\varepsilon}{\kappa_2} r_2^{(2)} (\mathbf{n} \cdot \nabla) \varphi_2 \tag{2.87h}$$

3. Numerical experiments

In this chapter, we briefly comment on some of the results that we have obtained during numerical experiments. Our vision was to show that the $\mathrm{SP_n}$ equations are indeed viable resources for modeling heat transport when radiation is counted in.

In this paper, we discuss only experiments done on a simple 1D problem. The setting can be interpreted as an infinite slab enclosed between two plains, $x = 0$ and $x = 1$, in 3D space. Since this slab domain is infinite in y and $z-$direction and we start from a homogeneous initial condition, the temperature evolution and intensity field do not depend on those coordinates. The temperature and intensity functions have nontrivial dependence only on one spatial variable along the x-axes. Thus the problem reduces into 1D problem.

3.1 One-domain setting

The basic setup is the one where our domain is formed by one medium $\mathcal{M}_1$ with constant refractive index n_1 and constant thermal conductivity k. The surrounding medium $\mathcal{M}_b$ has refractive index n_b and emits blackbody-like radiation B_b corresponding to fixed temperature T_b. Coefficients k_b and κ_b for $\mathcal{M}_b$ are irrelevant since we do not consider bulk equations to govern temperature in its volume.

The medium $\mathcal{M}_1$ is originally at constant temperature T_0 and then let cool down.

We have implemented a script for solving radiative heat transport problem by Rosseland approximation ((2.21a)) and also $\mathrm{SP_1}$ equations ((2.17), (2.18)). *Walfram Mathematica 13.0.1* has been the software used for this purpose.

Before we jump to our results, there are some important notes about the implementation. We set up an equation for the function $\varphi = \varphi(\mathbf{x}, t)$ with only spatial and time dependency, no frequency. It resembles the total energy flux defined at the beginning of section 2, it just does not take frequencies from the opaque band into account.

$$\varphi(\mathbf{x}, t) = \int_{\nu_1}^{\infty} \varphi(\mathbf{x}, t, \nu)\, d\nu \tag{3.1}$$

By this, we create an auxiliary function, with fewer arguments. However, for this averaging to be valid in our equations, the coefficient κ, which also appears inside the integral (see (2.87a)), needs to be constant.

For more accurate results we have the option of introducing several spectral bands (ν_i, ν_{i+1}), assigning each one with different κ_{ν_i} coefficient and defining separate intensity functions φ_{ν_i}. The coupling is then realized via their sum.

$$\frac{\partial T(\mathbf{x}, t)}{\partial t} = \nabla \cdot (k \nabla T(\mathbf{x}, t)) + \sum_i \nabla \cdot \frac{1}{3\kappa_i} \nabla \varphi_{\nu_i}(\mathbf{x}, t) \tag{3.2}$$

In the article (Larsen et al. [2003]) authors use 8 frequency bands to properly capture the behaviour of molten glass.

3.1.1 Rosseland approximation implementation

For the Rosseland equation, which is really just a single partial differential equation, the implementation was fairly straightforward.

In this approximation, we have eliminated the function φ from calculations and we consider radiation $B(\nu, T)$ instead. For this case, we also work with an average over the transparent spectrum. The expression

$$\int_{\nu_1}^{\infty} B(\nu, T)\, d\nu \tag{3.3}$$

can be precalculated as a function of $T(\mathbf{x}, t)$.

As for the actual solving technique, we employed the standard *NDSolveValue* function that was able to deal with a nonlinear partial differential equation with nontrivial mixed boundary condition. For the discretization, we set the solver to use so-called *Method of lines*. There were not many obstacles during these tests, we have kept the discretization at the default setting with spacing between grid points $\Delta x = 0.01$m and time step $\Delta t = 0.000\,01$s.

We have conducted a couple of numerical tests and compared our results to benchmark from the literature (Larsen et al. [2003]).

Here is a list of values for every coefficient needed.

- $T_b = 300\,\mathrm{K}$, $T_0 = 1000\,\mathrm{K}$, $k = 1\,\mathrm{W{\cdot}m^{-1}{\cdot}K^{-1}}$, $h = 1\,\mathrm{W{\cdot}m^{-2}{\cdot}K^{-1}}$, $n_1 = 1.46$, $n_b = 1$, $\nu_1 = 4.28 \cdot 10^{13}\,\mathrm{Hz}$, $\nu_2 = 9.99 \cdot 10^{13}\,\mathrm{Hz}$, $\alpha = 0.92$, $\varepsilon = 1$

It is quite a peculiar fact that our allegedly small parameter ε is not in fact that small. It is true that the smaller parameter ε is, the more sensitive and unstable the solving process gets. Plus as it turns out, even approximating with quite large ε value (≈ 1) gives quite satisfying results. After all, the $\mathrm{SP_n}$ and Rosseland equations can be derived without an asymptotic approach (McClarren [2010]; Brantley and Larsen [2000]).

Note that we are still to specify the κ coefficient. In our experiments, we have varied this parameter according to the article (Larsen et al. [2003]) to be able to compare the results. Here we actually computed with the two-band scheme, hence the frequency ν_2 listed among the coefficients. For each experiment we choose different κ_{ν_1} for frequencies from (ν_1, ν_2) and κ_{ν_2} for the rest from (ν_2, ∞).

In the following graphs that have been adopted from the article (Larsen et al. [2003]), we can see the data, the temperature functions, as presented in the literature, including original plot legends. Our results are depicted with **thick dashed red line**. The coincidence between their and our Rosseland outcomes is quite good, thus the graphs overlap and are harder to see.

What is actually being displayed is temperature distribution in studied interval $(0, 1)$, a cross-section of the slab, at time $t_{max} = 0.001\,\mathrm{s}$.

Although it may seem like everything worked out perfectly, there is one little glitch. The agreement between our results and the benchmark shown in figures from 3.1 to 3.5 only holds, if we set all blackbody radiation B, even in medium $\mathcal{M}_1$, to be equal to B_b associated with $n_b = 1$, in other words, the same refractive index $n = 1$ was used both for the external and internal medium

$$B = 1^2 \frac{2h_P\nu^3}{c_0^2} \frac{1}{e^{\frac{h_P\nu}{k_B T}} - 1}, \qquad \text{as oppose to} \qquad B = n_1^2 \frac{2h_P\nu^3}{c_0^2} \frac{1}{e^{\frac{h_P\nu}{k_B T}} - 1} \tag{3.4}$$

After carefully checking our code, we are convinced that in the considered reference, the authors computed with a different setting than the one claimed.

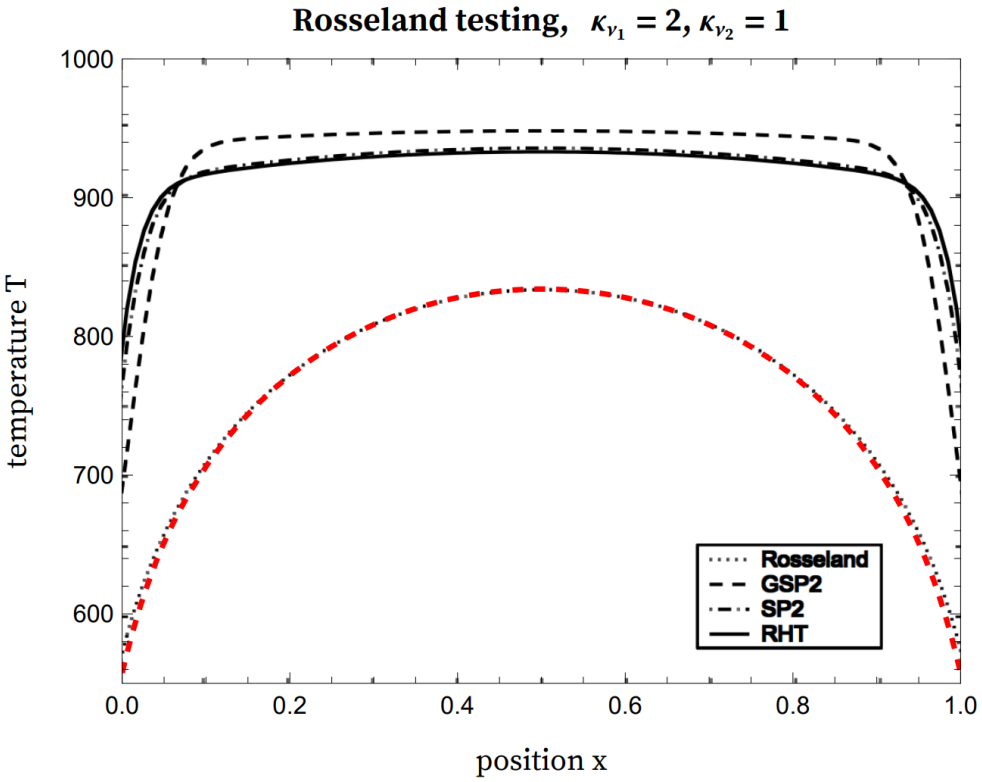

Figure 3.1: Test of heat transport in slab geometry - Rosseland equations - Temperature (T[K]) distribution (x[m]) at $t = 0.001\,\mathrm{s}$ for $\kappa_{\nu_1} = 2\,\mathrm{m}^{-1}$, $\kappa_{\nu_2} = 1\,\mathrm{m}^{-1}$

3.1.2 SP_1 equations implementation

The next challenge was to test the more complex diffusive model, SP_1 derived in this paper. These equations, although they are themselves approximation to (RTE), do carry a lot of difficulties. Compared to Rosseland, we now face a system of nonlinear partial differential equations with complicated boundary conditions.

We are able to get rid of the frequency dependence according to (3.1) and (3.2), this time with only one spectral band. However, a simple method of lines does not suffice. Here we had to engage a more sophisticated approach to solving this system and we have implemented so-called Rothe's method for the discretization of the PDE.

First, let us analyze the system at our hands. The bulk equations (2.87a) and (2.87b) are different in nature. The first one is a parabolic evolutionary equation for temperature, on the other hand, the second one is a stationary elliptic equation determining the distribution of intensity. Due to their coupling, we are forced to solve them simultaneously.

This might give us an idea to discretize the time variable and obtain two stationary equations with unknown functions dependent only on spatial variables. Now our system consists of two elliptic equations that can be solved subsequently for each time level.

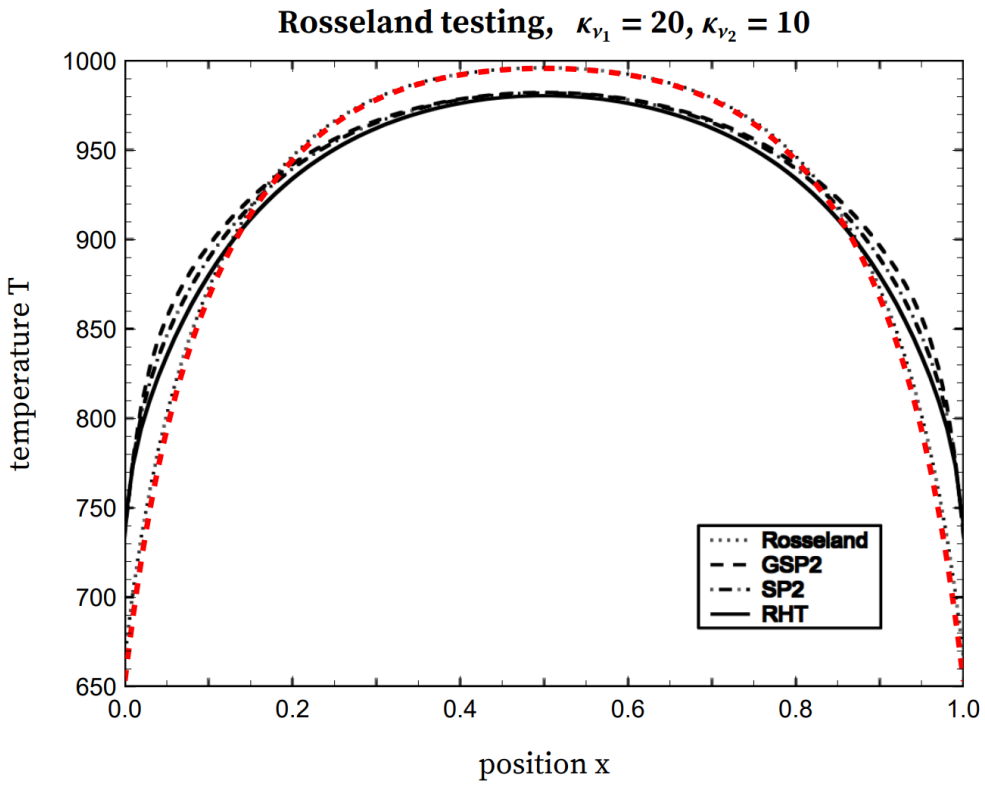

Figure 3.2: Test of heat transport in slab geometry - Rosseland equations - Temperature (T[K]) distribution (x[m]) at $t = 0.001\,\mathrm{s}$ for $\kappa_{\nu_1} = 20\,\mathrm{m}^{-1}$, $\kappa_{\nu_2} = 10\,\mathrm{m}^{-1}$

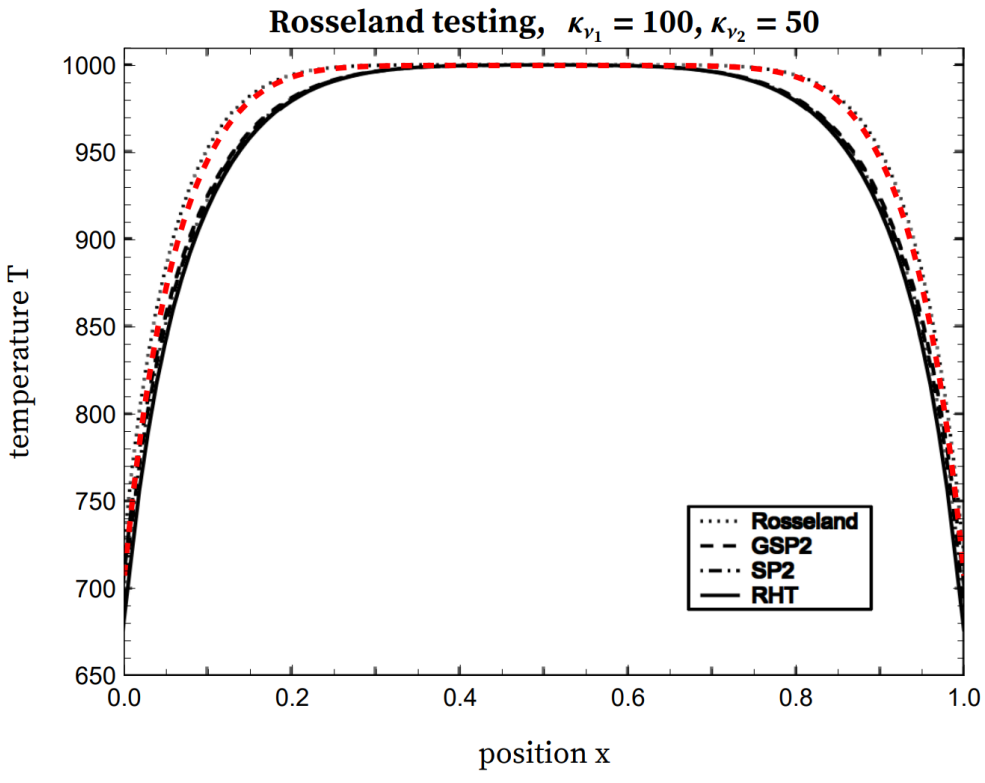

Figure 3.3: Test of heat transport in slab geometry - Rosseland equations - Temperature (T[K]) distribution (x[m]) at $t = 0.001\,\mathrm{s}$ for $\kappa_{\nu_1} = 100\,\mathrm{m}^{-1}$, $\kappa_{\nu_2} = 50\,\mathrm{m}^{-1}$

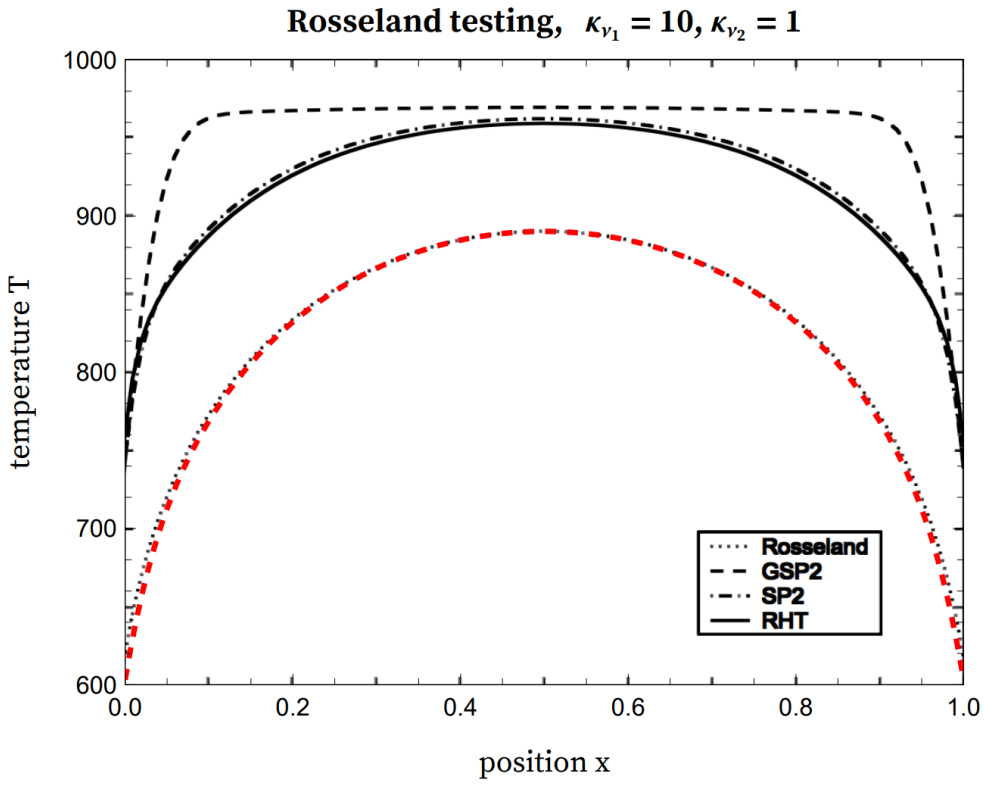

Figure 3.4: Test of heat transport in slab geometry - Rosseland equations - Temperature (T[K]) distribution (x[m]) at $t = 0.001\,\mathrm{s}$ for $\kappa_{\nu_1} = 10\,\mathrm{m}^{-1}$, $\kappa_{\nu_2} = 1\,\mathrm{m}^{-1}$

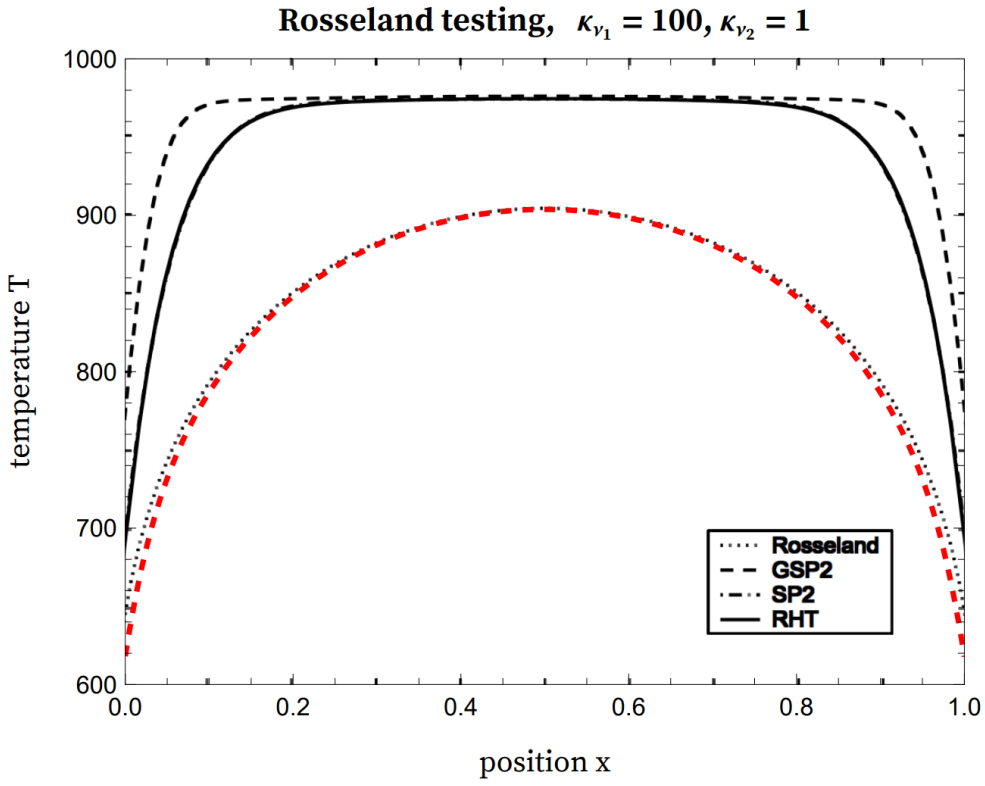

Figure 3.5: Test of heat transport in slab geometry - Rosseland equations - Temperature (T[K]) distribution (x[m]) at $t = 0.001\,\mathrm{s}$ for $\kappa_{\nu_1} = 100\,\mathrm{m}^{-1}$, $\kappa_{\nu_2} = 1\,\mathrm{m}^{-1}$

Let us denote $T_j(\mathbf{x})$ the temperature function at time t_j (j-th time level) and analogously $\varphi_j(\mathbf{x})$ the intensity function. The discretized (in time) form of the SP1 system then reads:

$$-\varepsilon^2\nabla\cdot\frac{1}{3\kappa}\nabla\varphi_j(\mathbf{x})+\kappa\varphi_j(\mathbf{x})=\kappa\int_{\nu_1}^{\infty}4\pi B(\nu,T_j)\,d\nu \qquad \text{for } \mathbf{x}\in\mathcal{M}_1=(0,1) \tag{3.5a}$$

$$\begin{aligned}\left(1-2r_1^{(1)}\right)\varphi_j(\mathbf{x})+\frac{2\varepsilon}{3\kappa}\left(1+3r_1^{(2)}\right)(\mathbf{n}\cdot\nabla)\varphi_j(\mathbf{x})=\\ =\left(1-2r_2^{(1)}\right)\int_{\nu_1}^{\infty}4\pi B_b(\nu,T_b)\,d\nu \qquad \text{for } \mathbf{x}\in\partial\mathcal{M}_1=\{0,1\}\end{aligned} \tag{3.5b}$$

$$\frac{T_{j+1}(\mathbf{x})-T_j(\mathbf{x})}{\Delta t}=\nabla\cdot(k\nabla T_{j+1}(\mathbf{x}))+\nabla\cdot\frac{1}{3\kappa}\nabla\varphi_j(\mathbf{x}) \qquad \text{for } \mathbf{x}\in\mathcal{M}_1=(0,1) \tag{3.6a}$$

$$\begin{aligned}\varepsilon k(\mathbf{n}\cdot\nabla)T_{j+1}(\mathbf{x})=h\left(T_b-T_{j+1}(\mathbf{x})\right)+\\ +\alpha\pi\int_0^{\nu_1}B_b(\nu,T_b)-B_b(\nu,T_j(\mathbf{x}))\,d\nu \qquad \text{for } \mathbf{x}\in\partial\mathcal{M}_1=\{0,1\}\end{aligned} \tag{3.6b}$$

Here the equations are in atypical order with intensity equations first and temperature second, but it is only natural like that because it is the way they have to be computed. Starting with $T_0(\mathbf{x})\equiv T_0$, we are able to obtain function $\varphi_0(\mathbf{x})$. This function is then used to complete the equation for temperature $T_1(\mathbf{x})$ and this process repeats. To solve equations (3.5a) and (3.6a), function *NDSolveValue* uses *Finite Element Method*.

First, we conducted two experiments to replicate the benchmark that was published in the article (Larsen et al. [2002]). The parameters are set to

- $T_b=300\,\mathrm{K}$, $T_0=1000\,\mathrm{K}$, $k=1\,\mathrm{W{\cdot}m^{-1}\cdot K^{-1}}$, $h=1\,\mathrm{W{\cdot}m^{-2}\cdot K^{-1}}$, $n_1=1.46$, $n_b=1$, $\nu_1=4.28\cdot10^{13}\,\mathrm{Hz}$, $\alpha=0.92$, $r_1^{(1)}=0.285574$, $r_1^{(2)}=0.145208$, $r_b^{(1)}=0.04293$, $\kappa=1\,\mathrm{m^{-1}}$

This time we limit ourselves only to one spectral band (ν_1,∞), but on the other hand, between the experiments we alter parameter ε from value 1 to 0.01. The first case is similar to the setting for Rosseland tests, the latter models optically thick diffusive environment.

Same as before, we observe the temperature distribution at time $t_{max}=0.001\,\mathrm{s}$. One of the reasons for the more complicated implementation of Rothe's method was the option of properly regulating the resolution of our computational grid.

In the case with $\varepsilon=1$, there was no need to make any alternations, we stuck with $\Delta=0.000\,01\,\mathrm{s}$, thus needed 100 time steps to reach t_{max}. We also kept the grid spacing at $\Delta x=0.01\mathrm{m}$.

We can see in figure 3.6 that again we managed to obtain quite nice looking results (our result is **thick dashed blue line**) coinciding with data from literature although we still face the unclarity regarding the refractive index n_1, ((3.4)).

In figure 3.7 we also display the distribution of auxiliary intensity function $\varphi(\mathbf{x})$, everything is symmetric as was expected.

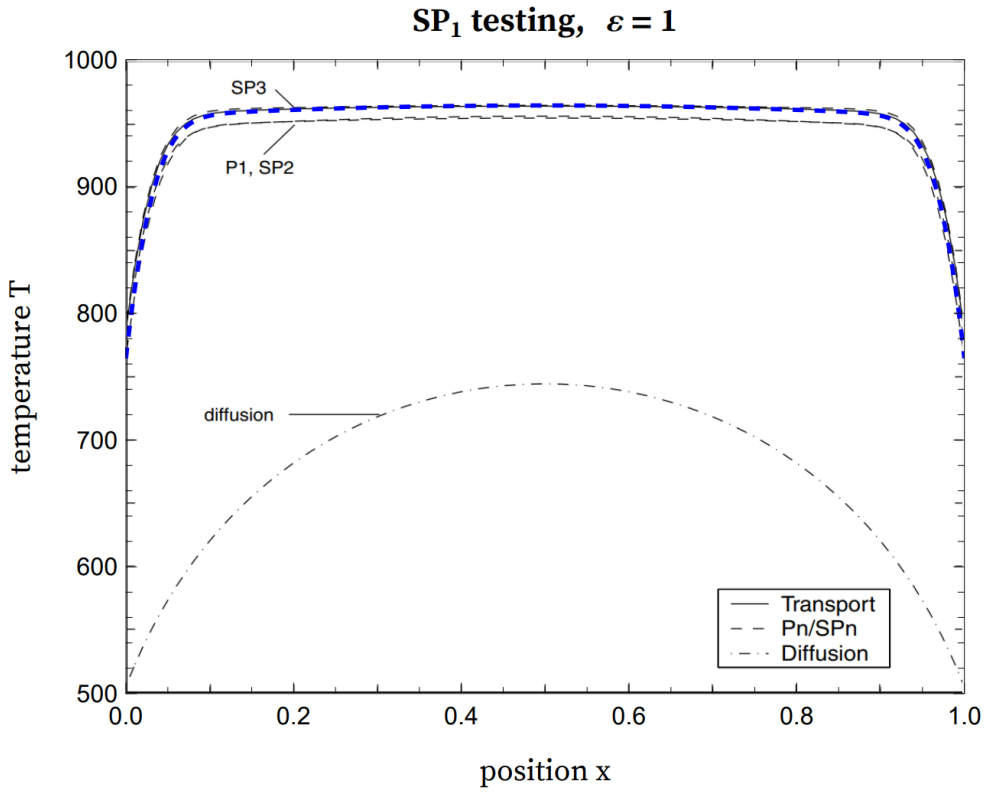

Figure 3.6: Test of heat transport in slab geometry - SP_1 equations - Temperature (T[K]) distribution (x[m]) at $t = 0.001\,\mathrm{s}$ for $\varepsilon = 1$

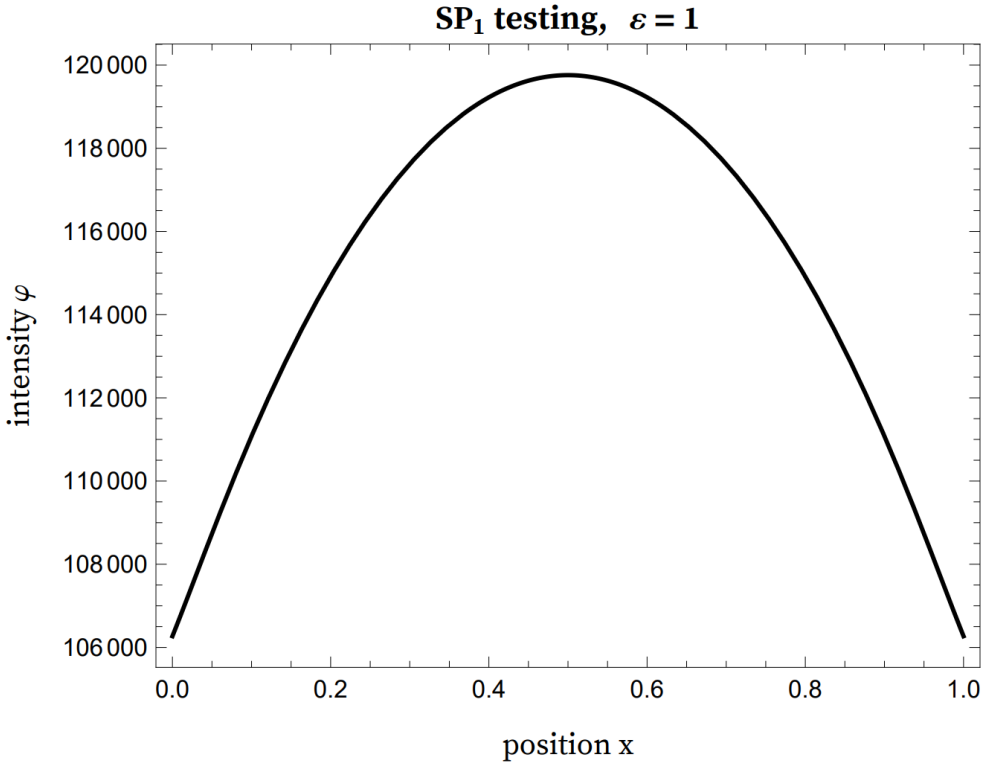

Figure 3.7: Test of heat transport in slab geometry - SP_1 equations - Intensity ($\varphi[\mathrm{J{\cdot}m^{-2}\cdot s^{-1}}]$) distribution ($x$[m]) for $\varepsilon = 1$

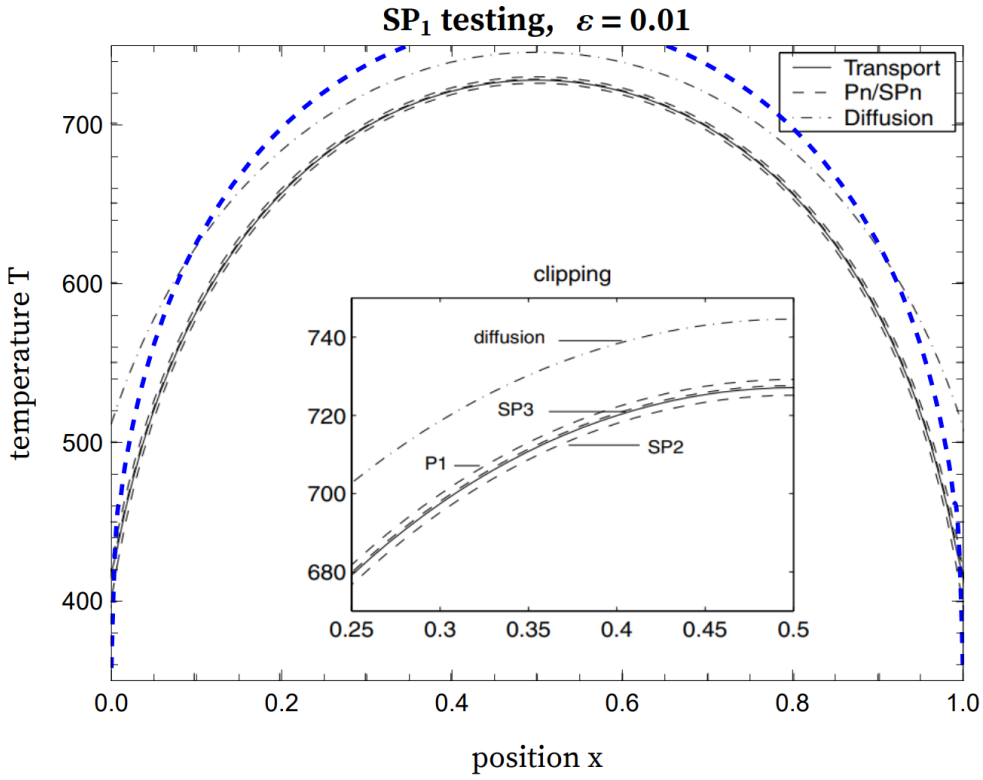

Figure 3.8: Test of heat transport in slab geometry - SP_1 equations - Temperature (T[K]) distribution (x[m]) at $t = 0.001$ s for $\varepsilon = 0.01$

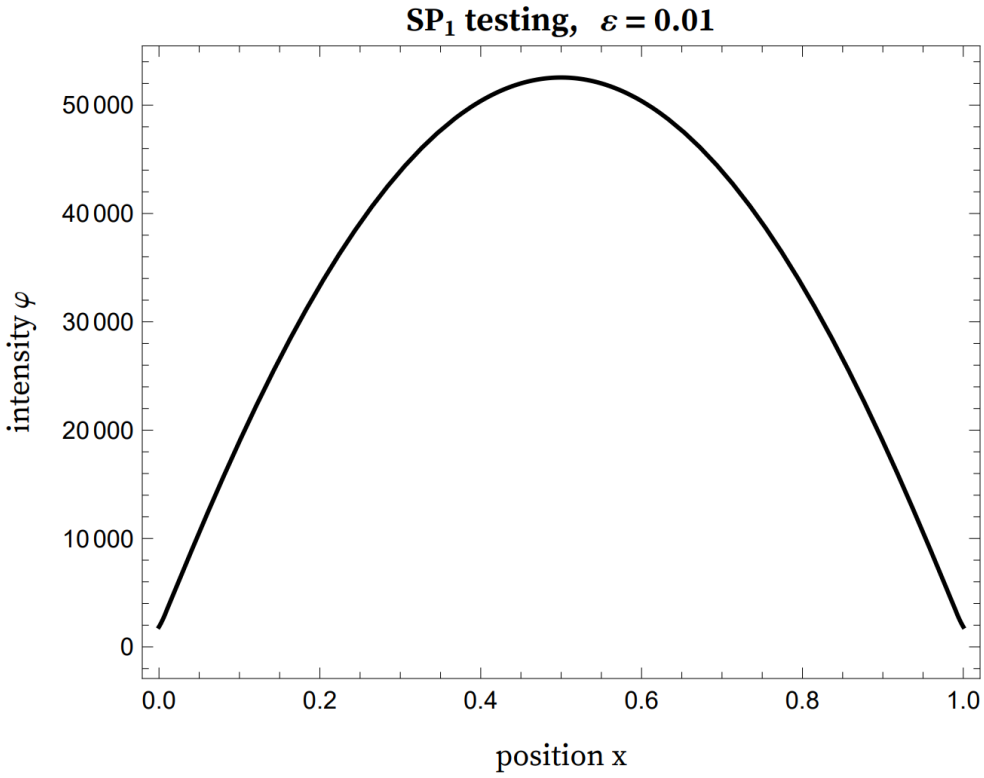

Figure 3.9: Test of heat transport in slab geometry - SP_1 equations - Intensity (φ[J·m^{-2} · s^{-1}]) distribution (x[m]) for $\varepsilon = 0.01$

When we decreased the value $\varepsilon = 0.01$, numerical calculations were not as smooth anymore. To get the solver output proper result we had to dramatically shorten our time step to $\Delta t = 0.000\,000\,2\,\mathrm{s}$, thus requiring 5000 time steps to finish. Axel Klar in paper (Klar et al. [2005], p. 1021) describes also similar experience. Yet, the solution does not match the benchmark perfectly, though it is similar in nature, see figure 3.8. As the published results only contain the temperature fields, and do not show the intensity, we have been unable to identify the source of the mismatch between our results and the published ones.

We again add also a graph of intensity $\varphi(\mathbf{x})$, see figure 3.9.

3.2 Two-domain setting

In this section, we present experiments with settings where the domain is divided into two parts with different optical properties. We are getting closer to the desired setup that replicates an industrial setting of molten glass surrounded by nitrogen.

3.2.1 SP_1 equations implementation

We proceed with using our implemented Rothe's method for the discretization of given SP_1 equations.

The first set of tests is calculated with just spatially dependent absorption coefficient κ. To be precise, we consider κ to be a piecewise constant function with one step at the middle of our domain interval. The results for this case are also provided in (Larsen et al. [2002]). Here we do not consider refractive indices to differ from one another, in other words, we set them both at value $n_1 = 1.46$. We can still use equations (3.5a)-(3.6b) mentioned above, no transition conditions required just yet.

All the parameters are listed here:

- $T_b = 300\,\mathrm{K}$, $T_0 = 1000\,\mathrm{K}$, $k = 1\,\mathrm{W{\cdot}m^{-1}\cdot K^{-1}}$, $h = 1\,\mathrm{W{\cdot}m^{-2}\cdot K^{-1}}$, $n_1 = n_2 = 1.46$, $n_b = 1$, $\nu_1 = 4.28 \cdot 10^{13}\,\mathrm{Hz}$, $\alpha = 0.92$, $r_1^{(1)} = 0.285574$, $r_1^{(2)} = 0.145208$, $r_b^{(1)} = 0.04293$, $\varepsilon = 0.1$
- $\kappa_1 = 0.1\,\mathrm{m^{-1}}$ for $x \in (0, 0.5)$, $\kappa_2 = 1\,\mathrm{m^{-1}}$ for $x \in (0.5, 1)$

In this simulation we again had to adjust the time step size appropriately according to ε, this instant we got by with $\Delta t = 0.000\,001\mathrm{s}$ needing 1000 time steps, similar to (Klar et al. [2005], p. 1021). Grid spacing is still the same, equidistant with $\Delta x = 0.01$.

In figure 3.10, we can see again that our solution is not exactly matching with those from the article (Larsen et al. [2002]) but is similar in nature, the reason could be (3.4) or other confusion about the parameters, for instance, t_{max} listed in that article is 0.01s instead of 0.001s. However, if we compare for example the values of Rosseland approximation with the ones from (Larsen et al. [2003]) where it is stopped at $t_{max} = 0.001\mathrm{s}$, there are only minor differences for which we give credits to distinct band division. Ten times longer time span would change the results significantly more.

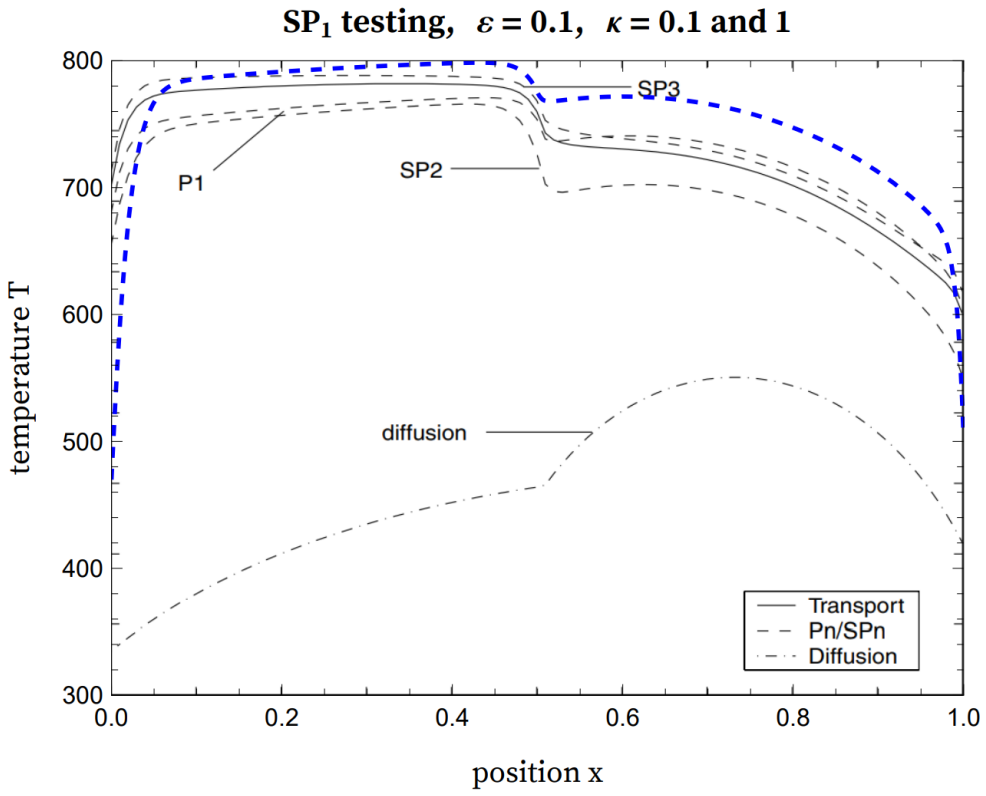

Figure 3.10: SP_1 equations - discontinuous κ - Temperature (T[K]) distribution (x[m]) at $t = 0.001\,\mathrm{s}$ for $\kappa_1 = 0.1\,\mathrm{m}^{-1}$ on (0, 0.5) and $\kappa_2 = 1\,\mathrm{m}^{-1}$ on (0.5, 1)

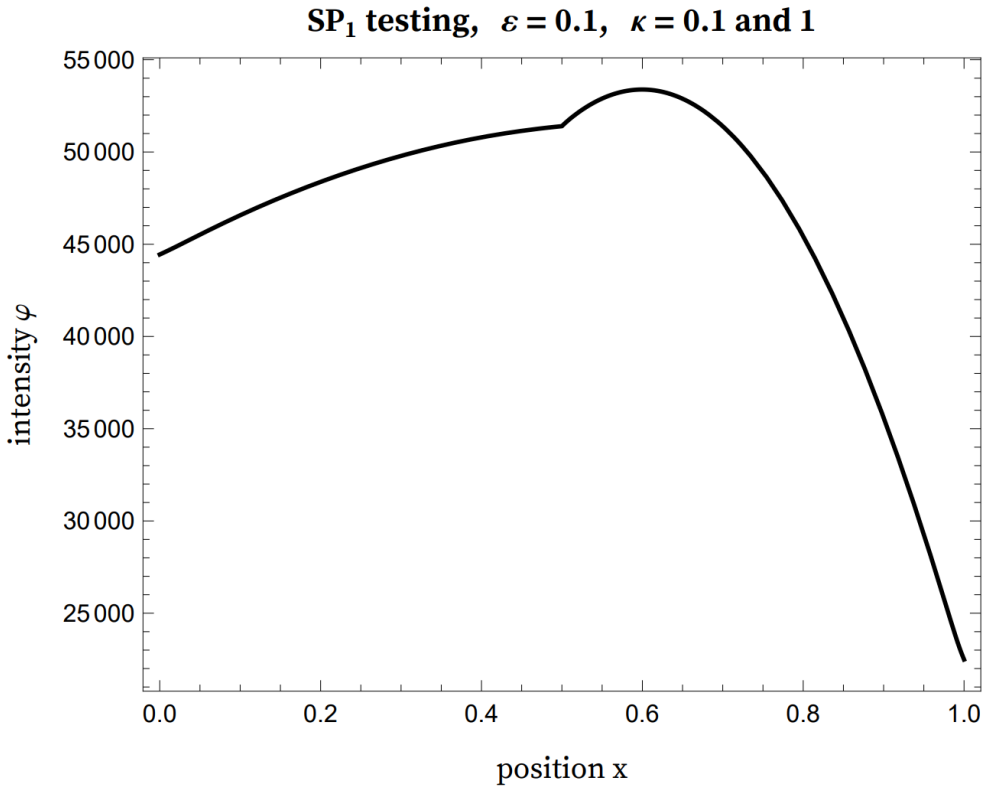

Figure 3.11: SP_1 equations - discontinuous κ - Intensity ($\varphi[\mathrm{J{\cdot}m^{-2}\cdot s^{-1}}]$) distribution ($x$[m]) at $t = 0.001\,\mathrm{s}$ for $\kappa_1 = 0.1\,\mathrm{m}^{-1}$ on (0, 0.5) and $\kappa_2 = 1\,\mathrm{m}^{-1}$ on (0.5, 1)

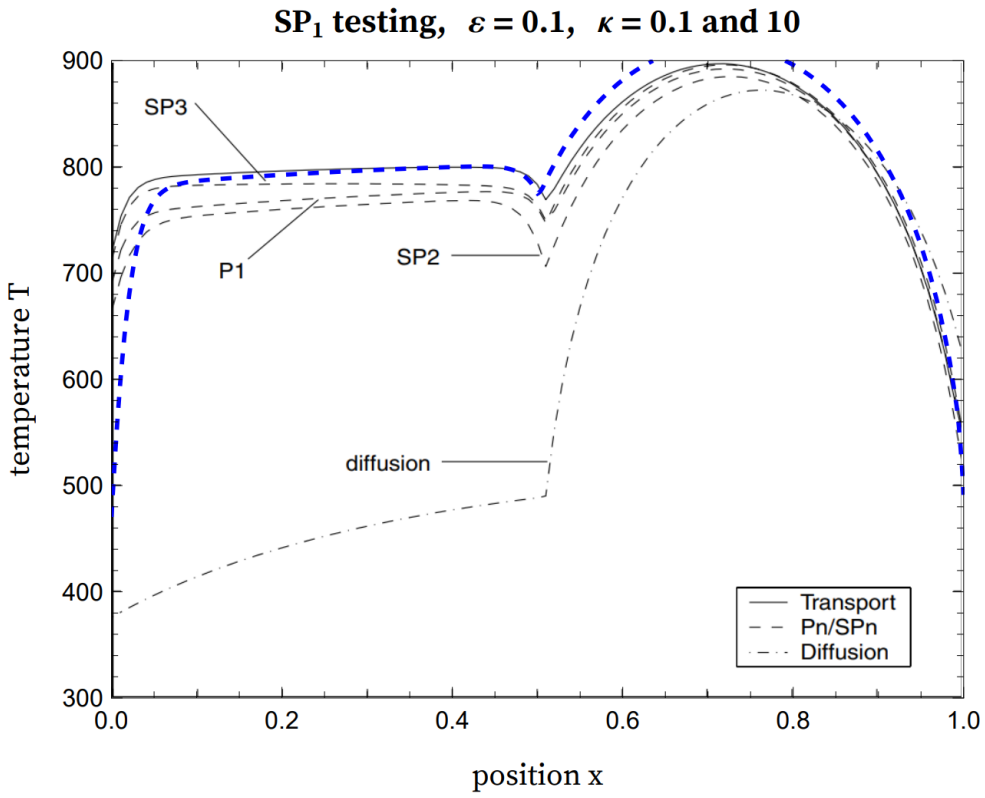

Figure 3.12: SP_1 equations - discontinuous κ - Temperature (T[K]) distribution (x[m]) at $t = 0.001\,\mathrm{s}$ for $\kappa_1 = 0.1\,\mathrm{m}^{-1}$ on (0, 0.5) and $\kappa_2 = 10\,\mathrm{m}^{-1}$ on (0.5, 1)

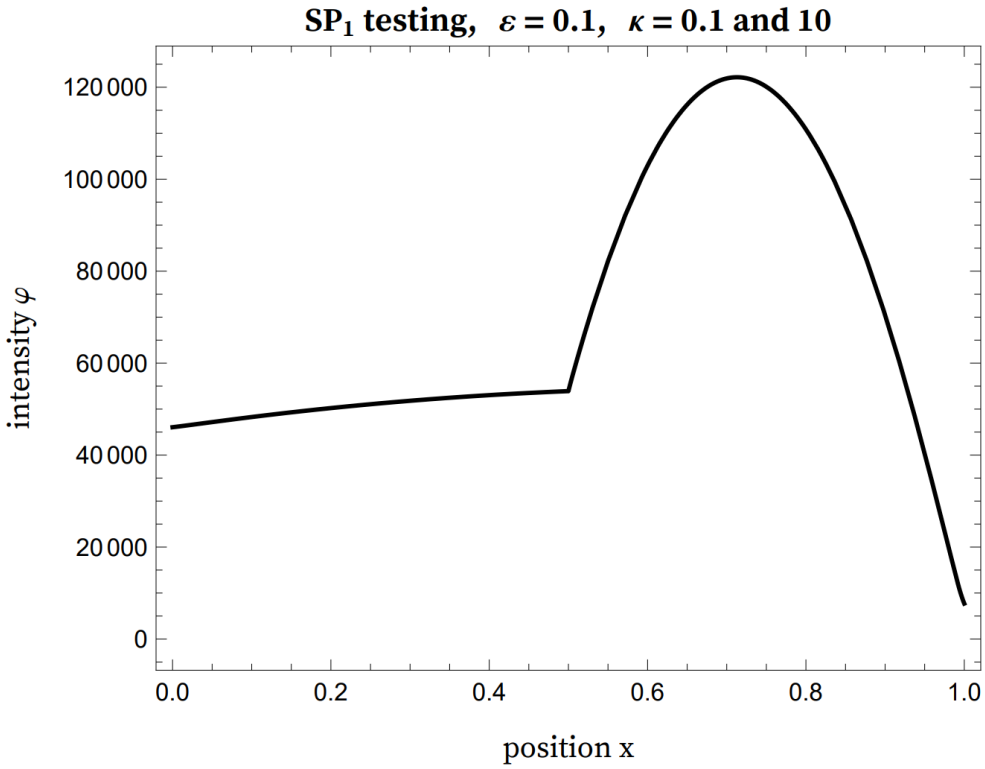

Figure 3.13: SP_1 equations - discontinuous κ - Intensity (φ[J·m^{-2}·s^{-1}]) distribution (x[m]) at $t = 0.001\,\mathrm{s}$ for $\kappa_1 = 0.1\,\mathrm{m}^{-1}$ on (0, 0.5) and $\kappa_2 = 10\,\mathrm{m}^{-1}$ on (0.5, 1)

We provided again an intensity distribution, figure 3.11. Since $\varphi(\mathbf{x})$ as an average over a sphere is a mere auxiliary function we do not have intuitive expectations on how it should behave at problematic spots like points of discontinuity of a parameter.

Here, we are delighted to see that the behavior is exactly what we expected. Since there is no jump in refractive indices, the SP_1 transition conditions reduce to form (2.85) and (2.86). We observe that the function is indeed continuous at the boundary and its left and right derivatives are proportional to the coefficient κ on each side.

A very similar simulation is shown in figures 3.12 and 3.13 with altered κ_2 coefficient.

- $\kappa_1 = 0.1\,\mathrm{m}^{-1}$ for $x \in (0, 0.5)$, $\kappa_2 = 10\,\mathrm{m}^{-1}$ for $x \in (0.5, 1)$

3.2.2 Implementation with novel transition conditions

Finally, we present experiments considering two domains that differ from one another not only with κ coefficient but also with refractive index n. In this section, we employ derived transition conditions (2.83) and (2.84) just to test the numerical solvability of such a system and confirm that it produces solutions with a discontinuous intensity.

This system is again discretized according to Rothe's method. In each time step, we have to compute the intensity field and then, from that the temperature distribution.

The intensity field is now a bit tricky to calculate, since we have to implement conditions in the middle of our domain interval. In fact, we search for two unknown functions $\varphi_1(\mathbf{x})$ and $\varphi_2(\mathbf{x})$ in an interval half the length of the original, (0, 0.5). These functions are then connected next to each other to create a function on the interval (0, 1). This means that for φ_1, the transition conditions apply at point 0.5, whereas for φ_2 they apply at point 0.

Thus we obtain a system of elliptic partial differential equations with nonlocalized boundary conditions, which still can be solved with standard *NDSolveValue* function.

Since there is no need for us to try to fit some benchmark results with this experiment, because there are not any, we can set B_1 to its proper form (not one from (3.4)). The parameters were in this case set to:

- $T_b = 300\,\mathrm{K}$, $T_0 = 1000\,\mathrm{K}$, $k = 1\,\mathrm{W{\cdot}m^{-1}\cdot K^{-1}}$, $h = 1\,\mathrm{W{\cdot}m^{-2}\cdot K^{-1}}$, $\nu_1 = 4.28 \cdot 10^{13}\,\mathrm{Hz}$, $\varepsilon = 0.1$
- $\kappa_1 = 0.1\,\mathrm{m}^{-1}$ for $x \in (0, 0.5)$, $\kappa_2 = 1\,\mathrm{m}^{-1}$ for $x \in (0.5, 1)$
- $n_1 = 1.46$, $n_2 = 1.000\,3$, $n_b = 1$, $\alpha_1 = 0.92$, $\alpha_2 = 2$, $r_{b,1}^{(1)} = 0.04293$, $r_{1,b}^{(1)} = 0.285574$, $r_{1,b}^{(2)} = 0.145208$, $r_{1,2}^{(1)} = 0.28543$, $r_{1,2}^{(2)} = 0.1451$, $r_{2,1}^{(1)} = 0.0428973$, $r_{2,1}^{(2)} = 0.0191179$, $r_{2,b}^{(1)} = 0.00035$, $r_{2,b}^{(2)} = 6.662 \cdot 10^{-6}$, $r_{b,2}^{(1)} = 0.000\,049$

These sets of numbers can be quite confusing, hence the helpful figure 3.14 in which we see two slab domains, $\mathcal{M}_1$ and $\mathcal{M}_2$, in contact surrounded by thermal reservoir $\mathcal{M}_b$. There is a number of rays depicted, each denoted with reflectivity

corresponding to the boundary it is pointing at. These reflectivities are calculated with the help of Fresnel's equation (1.25) or (1.26). We have to pay attention to the notation, the first index stands for the medium from which the ray is coming and the second one stands for the medium on the other side of the boundary. And for moments $r^{(1)}_{1,2}$ etc., the same rule holds.

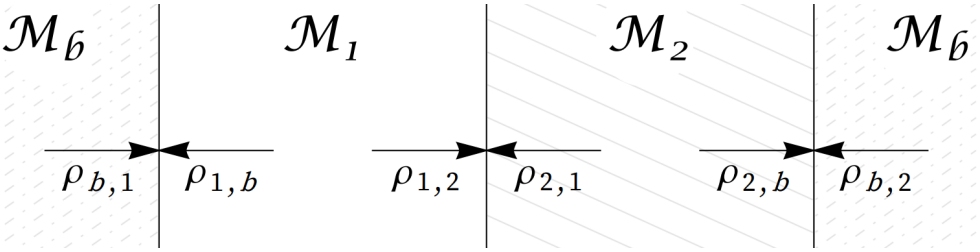

Figure 3.14: Scheme of two-domain setting

Brief comment dedicated to parameters α_1, resp. α_2: it is standard hemispherical emissivity used in temperature boundary condition at the interface between $\mathcal{M}_1$, resp. $\mathcal{M}_2$, and $\mathcal{M}_b$.

We have set $n_1 = 1.46$ and $n_2 = 1.0003$ to somewhat replicate the situation with molten glass mixture and surrounding nitrogen.

The graph in figure 3.15 carries some resemblance with the one in 3.10 but they are not completely the same. We can nicely see what difference changing the refractive index makes. Importantly, in figure 3.16 auxiliary intensity function is displayed. Clearly, the transition conditions force it to be discontinuous which does not necessarily mean the solution is wrong. In the last chapter, we discuss the possibility that the discontinuous solution may be the right answer to our problem.

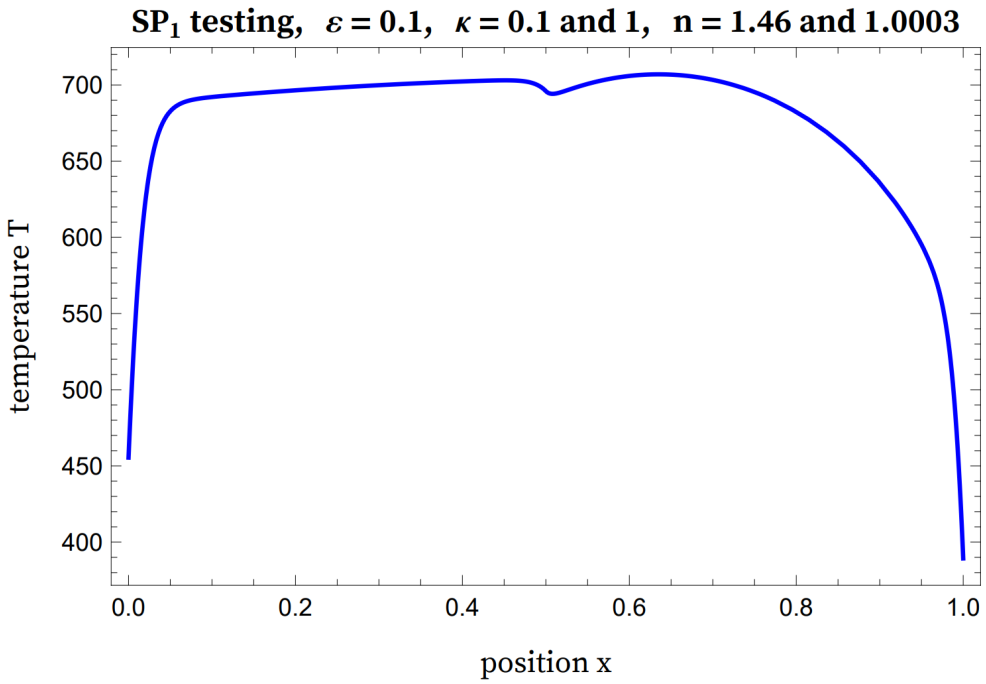

Figure 3.15: SP_1 equations - discontinuous κ and n - Temperature (T[K]) distribution (x[m]) at $t = 0.001\,\mathrm{s}$ for $\kappa_1 = 0.1\,\mathrm{m}^{-1}$, $n_1 = 1.46$ on (0, 0.5) and $\kappa_2 = 1\,\mathrm{m}^{-1}$, $n_2 = 1.000\,3$ on (0.5, 1)

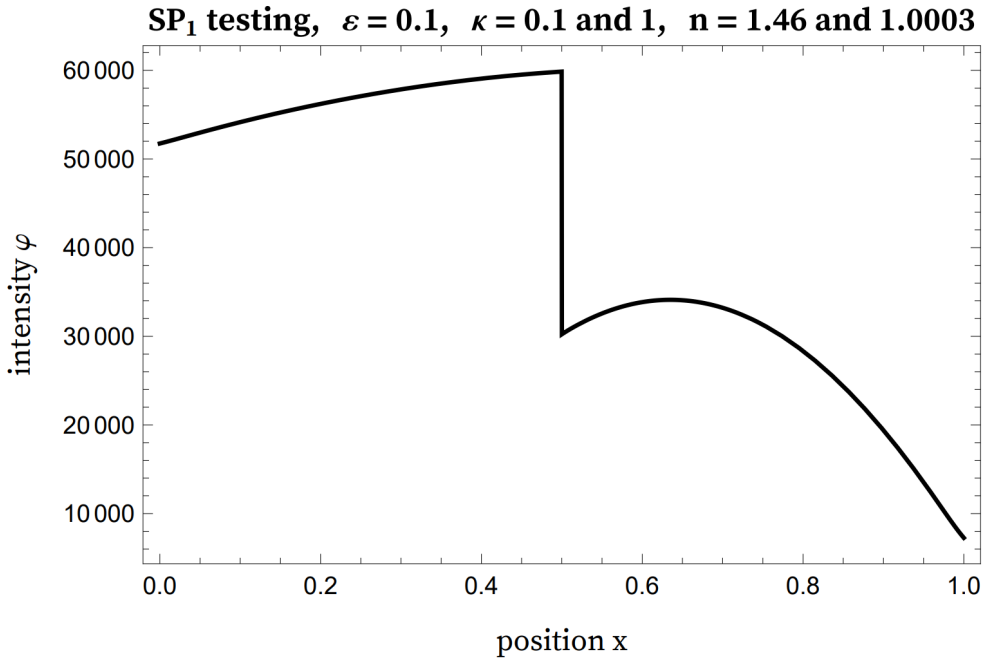

Figure 3.16: SP_1 equations - discontinuous κ and n - Intensity (φ[J·m^{-2} · s^{-1}]) distribution (x[m]) at $t = 0.001\,\mathrm{s}$ for $\kappa_1 = 0.1\,\mathrm{m}^{-1}$, $n_1 = 1.46$ on (0, 0.5) and $\kappa_2 = 1\,\mathrm{m}^{-1}$, $n_2 = 1.000\,3$ on (0.5, 1)

4. Discussion

After demanding derivations, approximations and testing, we have come to a part when it's time to stop for a while and think about current results and the direction of further efforts.

4.1 Qualitative analysis of SP_1 boundary and transition conditions

The SP_1 boundary and especially transition conditions are formulas probably not presented in the literature so far. It would be useful to convince ourselves that there is no fundamental problem with their application.

We have already noticed that for intensity average function $\varphi(\mathbf{x})$ they give us discontinuous solutions. Normally, this could be considered a red flag but not in this case. Let us take a look at the summarized system (2.87).

Usually, the first test of any complex system could be to investigate its stationary states, and whether they coincide with our expectations. It is only natural to assume that if the initial temperature T_0 is identical to the temperature of the outer reservoir T_b, then this state persists and no net energy transport occurs. Indeed, if we substitute $T_0 = T_b$ into our governing equations, then we get a trivial stationary solution $T_{st}(\mathbf{x}, t) \equiv T_b$.

First, we check that in such a scenario, intensity field φ_{st} in domain $\mathcal{M}_1$ with refractive index n_1 is constant with respect to space and time. Its value is

$$\varphi_{st}(\mathbf{x}, t, \nu) \equiv 4\pi \left(\frac{n_1}{n_b}\right)^2 B_b(\nu, T_b). \tag{4.1}$$

This function satisfies equation (2.87b) because

$$B(\nu, T_b) = \left(\frac{n_1}{n_b}\right)^2 B_b(\nu, T_b), \tag{4.2}$$

which follows straight from definition (1.7). The fact that φ_{st} fulfils also boundary condition (2.87f) can be deduced from relation (2.49) in special form

$$\left(\frac{n_1}{n_b}\right)^2 \left(1 - 2r_1^{(1)}\right) = \left(1 - 2r_b^{(1)}\right), \tag{4.3}$$

Since φ_{st} is constant in space, all the derivatives vanish from the equations and we are left with the aforementioned identities.

Similar reduction also happens in temperature equation (2.87a). There are only terms with derivatives so any constant solution satisfies this bulk equation. However, we need the exact temperature T_b to zero the right-hand side of boundary condition (2.87c).

We have convinced ourselves that functions T_{st} and φ_{st} are indeed stationary solutions in a one-domain setup. Now we proceed to the multi-domain arrangement and put our transition conditions to the test. We would like them to be consistent and allow for a similar type of stationary solution. It turns out that they do.

Let us consider a two-domain setup for simplicity. All we have to do is to define partial auxiliary intensity functions as constants in their domain:

$$\varphi_{st_1}(\mathbf{x}, t, \nu) \equiv 4\pi \left(\frac{n_1}{n_b}\right)^2 B_b(\nu, T_b) \tag{4.4a}$$

$$\varphi_{st_2}(\mathbf{x}, t, \nu) \equiv 4\pi \left(\frac{n_2}{n_b}\right)^2 B_b(\nu, T_b) \tag{4.4b}$$

We have already seen that these functions satisfy bulk and boundary equations, only left are the transition conditions (2.83) and (2.84). Since they are constants, the first one holds trivially and in the latter, we end up with identity (2.49) once again.

These conditions are therefore perfectly consistent with our expectations and we can conclude that in the case of different refractive indices, the auxiliary intensity variable φ must indeed be discontinuous.

4.2 SP_2 approximation

We have seen the derivation of boundary and transition conditions for a system of SP_1 equations. It raises the question, of whether an analogous procedure can be done also in the case of SP_2 equations, after all, they are quite similar.

In fact, it can be done and we have managed to find the right procedure by an asymptotic approach. The derivation itself is quite lengthy, thus here we provide just a brief outlook and present the results as curiosity without the full derivation, which may be presented in the future work.

Main nuance in the procedure is always taking more terms in asymptotic expansions, because SP_2 are higher order, particularly we need to use

$$I(\mathbf{\Omega}) = \left[1 - \frac{\varepsilon}{\kappa}(\mathbf{\Omega} \cdot \nabla) + \frac{\varepsilon^2}{\kappa^2}(\mathbf{\Omega} \cdot \nabla)^2\right] B \tag{4.5}$$

instead of (2.25). One more trick is required in final operations. Regarding the boundary conditions, to get the same formulation as presented in literature, we have neglect some terms of order $\mathcal{O}(\varepsilon^2)$,

$$\varepsilon^2 (\mathbf{n} \cdot \nabla)^2 B \approx \varepsilon^2 \nabla^2 B \tag{4.6}$$

thus we diminish the accuracy of our equations to achieve more pleasant form. This step can be somehow got around for the cost of more complex equations. However, we have not done any deeper analysis of this remark.

After fairly lengthy procedure, it is possible to obtain the final form of those equations.

SP_2 approximation

Bulk equations

$$\frac{\partial T(\mathbf{x},t)}{\partial t} = \nabla\cdot(k\nabla T(\mathbf{x},t)) \; + \\ + \int_{\nu_1}^{\infty} \nabla\cdot\frac{1}{3\kappa}\nabla\left[\varphi(\mathbf{x},t,\nu) + \frac{4}{5}\Big(\varphi(\mathbf{x},t,\nu) - 4\pi B(\nu,T)\Big)\right] d\nu \quad (4.7a)$$

$$-\varepsilon^2\nabla\cdot\frac{1}{3\kappa}\nabla\left[\varphi(\mathbf{x},t,\nu) + \frac{4}{5}\Big(\varphi(\mathbf{x},t,\nu) - 4\pi B(\nu,T)\Big)\right] + \\ + \kappa\varphi(\mathbf{x},t,\nu) = \kappa(4\pi B(\nu,T)) \quad (4.7b)$$

Temperature boundary condition

$$\varepsilon k(\mathbf{n}\cdot\nabla)T(\mathbf{x},t) = h\left(T_b - T(\mathbf{x},t)\right) + \alpha\pi\int_0^{\nu_1} B_b(\nu,T_b) - B_b(\nu,T)\,d\nu \quad (4.7c)$$

Temperature transition conditions

$$T_1(\mathbf{x},t) = T_2(\mathbf{x},t) \quad (4.7d)$$

$$k_1(\mathbf{n}\cdot\nabla)T_1(\mathbf{x},t) = k_2(\mathbf{n}\cdot\nabla)T_2(\mathbf{x},t) \quad (4.7e)$$

Intensity boundary condition

$$\left(1-2r_1^{(1)}\right)\varphi + \frac{2\varepsilon}{3\kappa}\left(1+3r_1^{(2)}\right)(\mathbf{n}\cdot\nabla)\left[\varphi + \frac{4}{5}\Big(\varphi - 4\pi B(\nu,T)\Big)\right] + \\ + \frac{1}{2}\left(1-12r_1^{(3)}+4r_1^{(1)}\right)\Big[\varphi - 4\pi B(\nu,T)\Big] = \left(1-2r_b^{(1)}\right)4\pi B_b(\nu,T_b) \quad (4.7f)$$

Intensity transition conditions

$$\frac{1}{\kappa_1}(\mathbf{n}\cdot\nabla)\left[\varphi_1 + \frac{4}{5}\Big(\varphi_1 - 4\pi B_1(\nu,T)\Big)\right] = \frac{1}{\kappa_2}(\mathbf{n}\cdot\nabla)\left[\varphi_2 + \frac{4}{5}\Big(\varphi_2 - 4\pi B_2(\nu,T)\Big)\right] \quad (4.7g)$$

$$\left(1-2r_1^{(1)}\right)\varphi_1 + \frac{2\varepsilon}{\kappa_1}r_1^{(2)}(\mathbf{n}\cdot\nabla)\left[\varphi_1 + \frac{4}{5}\Big(\varphi_1 - 4\pi B_1(\nu,T)\Big)\right] + \\ + \frac{1}{2}\left(1-12r_1^{(3)}+4r_1^{(1)}\right)\Big[\varphi_1 - 4\pi B_1(\nu,T)\Big] = \\ = \left(1-2r_2^{(1)}\right)\varphi_2 - \frac{2\varepsilon}{\kappa_2}r_2^{(2)}(\mathbf{n}\cdot\nabla)\left[\varphi_2 + \frac{4}{5}\Big(\varphi_2 - 4\pi B_2(\nu,T)\Big)\right] + \\ + \frac{1}{2}\left(1-12r_2^{(3)}+4r_2^{(1)}\right)\Big[\varphi_2 - 4\pi B_2(\nu,T)\Big] \quad (4.7h)$$

Conclusion

Let us recapitulate our goals and compare them with our achievements.

In the first part of the thesis, we successfully rederived the partial differential equations for the conductive and radiative heat transport between semi-transparent materials as presented in the numerous literature on the topic (Frank and Klar [2011]; Howell et al. [2021]). We recognized the complexity of this system and proceeded with approximation by relations with higher order diffusion operators, in other words, SP_n equations. Their derivation carefully followed asymptotic methods described in preceding articles (Frank and Klar [2011], Larsen et al. [2002]). To obtain a full system, we had to transform also the boundary conditions, where, in contrast to most other authors, we employed asymptotic methods. In the end, we generalized the boundary equation and obtained transition conditions describing the behaviour of the radiation field on the interface between two domains with different refractive indices.

During numerical experiments, we restricted ourselves only to 1D problems given the persisting complexity of the approximating governing system. We managed to test Rosseland approximation and SP_1 equations. There were some discrepancies between our and the benchmark results, thus we were able to match them only by considering different values for certain parameters. Naturally, this tinted our joy from the match, which turned out quite well (especially in Rosseland case) but since along the way, we had discovered more than one typo in the article providing the benchmark (Larsen et al. [2003]), the error could have been made by the authors of the benchmark.

Independently of the previous experiments, we also tested our new transition conditions. We showed, in particular, that they allow for numerical solvability of the arising system while providing solutions with discontinuous radiation intensity. We have provided a reasoning why such discontinuous solutions should be favorable compared to continuous ones.

In future work, we would like to employ our results regarding SP_2 equations mentioned in 4.2 and simulate proper glass cooling in 3D setting probably with different more suitable software.

Of course, there are still options for improvement and further research outside the scope of SP_n equations. The thermal radiation could be calculated by brute force with ray-tracing methods, those calculations are however extremely demanding and one has to engage certain numerical theory and a huge amount of computing power to pursue this case.

Bibliography

P. S. Brantley and E. W. Larsen. The simplified P3 approximation. *Nuclear Science and Engineering*, 134(1):1–21, 2000. doi: 10.13182/NSE134-01. URL https://doi.org/10.13182/NSE134-01.

M. Frank and A. Klar. Radiative heat transfer and applications for glass production processes. In A. Fasano, editor, *Mathematical models in the manufacturing of Glass, Lecture Notes in Mathematics*, pages 57–134. Springer, Berlin, 2011. URL https://doi.org/10.1007/978-3-642-15967-1_2.

John R. Howell, M. Pinar Mengüc, Kyle J. Daun, and Robert Siegel. *Thermal radiation heat transfer*. Seventh Edition. CRC Press, 2021. URL https://doi.org/10.1201/9780429327308.

A. Klar, J. Lang, and M. Seaïd. Adaptive solutions of SPN-approximations to radiative heat transfer in glass. *International Journal of Thermal Sciences*, 44: 1013–1023, 2005.

E. W. Larsen, G. Thömmes, A. Klar, M. Seaïd, and T. Götz. Simplified PN approximations to the equations of radiative heat transfer and applications. *Journal of Computational Physics*, 183(2):652–675, 2002. doi: 10.1006/jcph.2002.7210.

E. W. Larsen, G. Thömmes, and A. Klar. New frequency-averaged approximations to the equations of radiative heat transfer. *SIAM Journal on Applied Mathematics*, 64(2):565–582, 2003. URL https://www.jstor.org/stable/4096000.

C. Matyska. Mathematical introduction in geotherimcs and geodynamics, 2005. URL https://geo.mff.cuni.cz/studium/Matyska-MathIntroToGeothermicsGeodynamics.pdf.

R. G. McClarren. Theoretical aspects of the simplified Pn equations. *Transport Theory and Statistical Physics*, 39(2-4):73–109, 2010.

M. Řehoř, J. Blechta, and O. Souček. On some practical issues concerning the implementation of cahn-hilliard-navier-stokes type models. *International Journal of Advances in Engineering Sciences and Applied Mathematics*, 9(1):30–39, 2017.

List of Figures

A. Pilkinkton process

To closer introduce the topic to the reader and for the sake of better understanding, we first discuss the principles of flat-glass formation. This procedure, which is sometimes called *Pilkington process*, has been used in industry since 1950 when it was developed for the first time. Detailed description of the process can be found in article written by Pilkington himself.

The idea of this method is to melt the glass material to gain homogenous structure and then to pour it into a form, so it remolds into shape with absolutely flat faces. The clever trick inheres in the construction of the form. It is actually a bath with molten tin on the bottom whose surface is perfectly flat, thus creating very good base for the form. So, the molten glass mixture is emptied out of the furnace and poured onto a layer of molten tin. Then the "melded" mixture is let to settle, note that glass and tin are immiscible, thus making this step possible.

Then the cooling process starts. This part has a significant impact on the final product quality, meaning if the temperature is not lowered uniformly, the glass might be fragile and even cracking.

This method was developed and widely used because it guarantees a glass panel with completely flat surface and doesn't require any type of grinding or polishing.

A.1 Principles of glass forming procedure

What we consider general knowledge is that the glass is created from a molten mixture of specific materials, those being mainly silicon dioxide extracted from sand and potassium carbonate, else sodium carbonate, or limestone. The assortment is then heated up to around 1500°C so it melts to achieve a truly uniform structure of the resulting product.

Now that we have the molten glass mixture ready, we deal with a very simple problem with a nontrivial solution: How to form perfectly flat sheets of glass? Sir Alastair Pilkington came up with an ingenious answer to our question. He invented the aforementioned game-changing manufacturing procedure, later called after him, the Pilkington process. The molten mixture is poured out into a bath of molten tin. One might ask, why the bottom of the bath has to be liquid, it seems that it only increases the costs of energy for heating, plus it may be impractical and encumber any manipulation. On top of that, a liquid substances in their presence make the mechanical models really complicated.

One of the main advantages and reasons for the form to have liquid bottom is the perfect flatness. The liquid ensures not only that the surface alone is completely flat, but also the level is naturally in exact horizontal plane. This really effortlessly helps the molten glass mixture to have constant depth over the whole volume, as even the slightest tilt would cause the liquid to accumulate on one side of the form.

A.2 Cooling phase

One may think that the main part of glass production is over once we have melted the glass mixture and filled the appropriate form with it. However, the cooling phase is at the same level of importance, if not even higher. In any case, it is definitely the part that requires to be treated meticulously and with great caution.

During the cooling of the glass, our goal is to keep the temperature as uniform as possible. temperature heterogeneities lead to a formation of structures, internal mechanical tension and other defects leading to increased fragility of the product. The cooling process has to be slow and fully controlled.

In mathematical modelling of the Pilkington process, proper treatment of the thermal evolution is thus of utmost importance. The fact that both the gas and glass mediums are semi-transparent, together with the very high temperatures in the system, imply the necessity of considering radiative contribution to the heat transfer. From this point of view, this particular application presents a nice real-world example of a process where application of the methods presented in the thesis are necessary.

B. Integral formula

We provide proof of identity

$$\int_{S^2} (\boldsymbol{\Omega} \cdot \nabla)^n \, d\boldsymbol{\Omega} = [1 + (-1)^n] \, \frac{2\pi}{n+1} \nabla^n \tag{B.1}$$

that is crucial for derivation and yet many authors just use it without any comment on why it holds. Let us take a look at that integral that frequently appears in our equations.

$$\int_{S^2} (\boldsymbol{\Omega} \cdot \nabla)^n \, d\boldsymbol{\Omega} \tag{B.2}$$

We can express the product of n terms as tensor inner product and move the differential tensor out of the integral as the two operations commute

$$\int_{S^2} (\boldsymbol{\Omega} \cdot \nabla)^n \, d\boldsymbol{\Omega} = \int_{S^2} (\boldsymbol{\Omega} \otimes \boldsymbol{\Omega} \otimes \ldots \otimes \boldsymbol{\Omega}) \, d\boldsymbol{\Omega} : (\nabla \otimes \nabla \otimes \ldots \otimes \nabla) \tag{B.3}$$

Here we integrate a tensor one component at a time. Each of them consists of product of n components from $\boldsymbol{\Omega}$:

$$\int_{S^2} (\boldsymbol{\Omega} \otimes \boldsymbol{\Omega} \otimes \ldots \otimes \boldsymbol{\Omega})_{ij\ldots z} \, d\boldsymbol{\Omega} = \int_{S^2} \boldsymbol{\Omega}_i \boldsymbol{\Omega}_j \ldots \boldsymbol{\Omega}_z \, d\boldsymbol{\Omega} \tag{B.4}$$

where $i, j, \ldots, z \in \{1, 2, 3\}$. Now we introduce another trick into our calculation, we consider a special generating function $G(\mathbf{a}) = G((a_1, a_2, a_3))$:

$$G(\mathbf{a}) = \int_{S^2} e^{\mathbf{a} \cdot \boldsymbol{\Omega}} \, d\boldsymbol{\Omega} \tag{B.5}$$

It is easy to see that once we obtain this function G, we can write that integral from (B.4) is equal to:

$$\int_{S^2} \boldsymbol{\Omega}_i \boldsymbol{\Omega}_j \ldots \boldsymbol{\Omega}_z \, d\boldsymbol{\Omega} = \frac{\partial^n}{\partial a_i \partial a_j \ldots \partial a_z} G(\mathbf{a}) \bigg|_{\mathbf{a}=\mathbf{0}} \tag{B.6}$$

or in a more elegant way using multiindexes

$$\int_{S^2} \boldsymbol{\Omega}^{\boldsymbol{\alpha}} \, d\boldsymbol{\Omega} = \frac{\partial^{|\boldsymbol{\alpha}|}}{\partial \mathbf{a}^{\boldsymbol{\alpha}}} G(\mathbf{a}) \bigg|_{\mathbf{a}=\mathbf{0}}, \tag{B.7}$$

where $|\boldsymbol{\alpha}| = n$ and we use multiindex notation

$$\boldsymbol{\alpha} = (\alpha_1, \alpha_2, \alpha_3) \qquad \binom{n}{\boldsymbol{\alpha}} = \frac{n!}{\alpha_1! \alpha_2! \alpha_3!} \qquad \mathbf{a}^{\boldsymbol{\alpha}} = a_1^{\alpha_1} a_2^{\alpha_2} a_3^{\alpha_3} \tag{B.8}$$

Let us figure out the actual form of the function G then. We will expand the exponential inside into its Taylor series and then interchange the sum and integral to get:

$$G(\mathbf{a}) = \int_{S^2} \sum_{k=0}^{\infty} \frac{(\mathbf{a} \cdot \boldsymbol{\Omega})^k}{k!} \, d\boldsymbol{\Omega} = \sum_{k=0}^{\infty} \int_{S^2} \frac{(\mathbf{a} \cdot \boldsymbol{\Omega})^k}{k!} \, d\boldsymbol{\Omega} \tag{B.9}$$

Since there is spherical symmetry that can be taken advantage of, it does not really matter in which direction vector $\mathbf{a}$ is pointing. The result depends only on its magnitude. Without the loss of generality, we choose $\mathbf{a}$ to be in direction of the z-axis, $\mathbf{a} = \|\mathbf{a}\|\mathbf{e}_3$. Then it holds:

$$\int_{S^2} \frac{(\mathbf{a}\cdot\boldsymbol{\Omega})^k}{k!}\,d\boldsymbol{\Omega} = \frac{\|\mathbf{a}\|^k}{k!}\int_{S^2}(\mathbf{e}_3\cdot\boldsymbol{\Omega})^k\,d\boldsymbol{\Omega} = \frac{\|\mathbf{a}\|^k}{k!}\int_0^{2\pi}\int_0^{\pi}\cos^k(\theta)\sin(\theta)\,d\theta\,d\phi = \\ = 2\pi\frac{\|\mathbf{a}\|^k}{k!}\int_{-1}^{1}\mu^k\,d\mu = 2\pi\frac{\|\mathbf{a}\|^k}{k!}\frac{1}{k+1}\left(1+(-1)^k\right) \tag{B.10}$$

This expression is non-zero only for even values of k. We can quickly check the correctness of our result; odd-k terms vanish because they allow $(\mathbf{a}\cdot\boldsymbol{\Omega})^k$ to be positive on one hemisphere and negative on the other, thus canceling each other out.

We combine (B.9), (B.10) and the fact that $\|\mathbf{a}\|^2 = \mathbf{a}\cdot\mathbf{a}$ to get final form of $G(\mathbf{a})$:

$$G(\mathbf{a}) = \sum_{k=0}^{\infty} 4\pi\frac{(\mathbf{a}\cdot\mathbf{a})^k}{(2k+1)!} \tag{B.11}$$

Each term is a polynomial with variables a_1, a_2 and a_3 containing only summands with certain degree

$$(\mathbf{a}\cdot\mathbf{a})^k = \sum_{|\boldsymbol{\beta}|=k}\binom{2k}{2\boldsymbol{\beta}}\mathbf{a}^{2\boldsymbol{\beta}}, \tag{B.12}$$

Recall equation (B.7), we want to differentiate G function n times and then set $\mathbf{a} = \mathbf{0}$. Note that from the whole series (B.11), only terms where $2k = n$ have the chance of not vanishing once we proclaim $\mathbf{a} = \mathbf{0}$. They are those which stay constant after differentiating. So if there should end up at least one non-zero term, n must be even.

$$\frac{\partial^{|\boldsymbol{\alpha}|}}{\partial\mathbf{a}^{\boldsymbol{\alpha}}}\left[(\mathbf{a}\cdot\mathbf{a})^k\right] = \frac{\partial^{|\boldsymbol{\alpha}|}}{\partial\mathbf{a}^{\boldsymbol{\alpha}}}\sum_{|\boldsymbol{\beta}|=k}\binom{2k}{2\boldsymbol{\beta}}\mathbf{a}^{2\boldsymbol{\beta}} \tag{B.13}$$

Again, the only term left after differentiating is precisely one for which $\boldsymbol{\alpha} = 2\boldsymbol{\beta}$, because in the others we surpass with differentiating operator degree of some variable and get 0 (like when $\frac{\partial^4(x^2y^2)}{\partial x^4} = 0$). Therefore we get

$$\frac{\partial^{|2\boldsymbol{\beta}|}}{\partial\mathbf{a}^{2\boldsymbol{\beta}}}\binom{2k}{2\boldsymbol{\beta}}\mathbf{a}^{2\boldsymbol{\beta}} = \frac{\partial^{2k}}{\partial a_1^{2\beta_1}\partial a_2^{2\beta_2}\partial a_3^{2\beta_3}}\frac{(2k)!}{(2\beta_1)!(2\beta_2)!(2\beta_3)!}a_1^{2\beta_1}a_2^{2\beta_2}a_3^{2\beta_3} = (2k)! \tag{B.14}$$

We can conclude that if $n = 2k$, in other words, it is an even number, then

$$\frac{\partial^{2k}}{\partial\mathbf{a}^{2\boldsymbol{\beta}}}G(\mathbf{a})\Big|_{\mathbf{a}=\mathbf{0}} = 4\pi\frac{(2k)!}{(2k+1)!} = \frac{4\pi}{2k+1} \tag{B.15}$$

otherwise (n odd) it evaluates to 0. On top of that, the multiindex $\boldsymbol{\alpha}$ from (B.7) has to be in the form of $\boldsymbol{\alpha} = 2\boldsymbol{\beta}$. Thus in tensor $\int_{S^2}(\boldsymbol{\Omega}\otimes\boldsymbol{\Omega}\otimes\ldots\otimes\boldsymbol{\Omega})\,d\boldsymbol{\Omega}$,

only components whose coordinates contain every index even number of times are non-zero. Once we then apply the inner product, it simplifies to

$$\int_{S^2} (\mathbf{\Omega} \otimes \mathbf{\Omega} \otimes \ldots \otimes \mathbf{\Omega})\, d\mathbf{\Omega} : (\nabla \otimes \nabla \otimes \ldots \otimes \nabla) = \frac{4\pi}{2k+1} \sum_{|\beta|=k} \binom{2k}{2\boldsymbol{\beta}} \frac{\partial^{2k}}{\partial \mathbf{x}^{2\beta}} = \\ = \frac{4\pi}{2k+1} (\nabla \cdot \nabla)^k \tag{B.16}$$

Thus we can write for any $n \in \mathbb{N}$

$$\int_{S^2} (\mathbf{\Omega} \cdot \nabla)^n \, d\mathbf{\Omega} = [1 + (-1)^n] \, \frac{2\pi}{n+1} \nabla^n \tag{B.17}$$